

Efficient Intramolecular Hydroalkoxylation of Unactivated Alkenols Mediated by Recyclable Lanthanide Triflate Ionic Liquids: Scope and Mechanism

Alma Dzudza^[b] and Tobin J. Marks^{*[a]}

Abstract: Lanthanide triflate complexes of the type $[\text{Ln}(\text{OTf})_3]$ ($\text{Ln} = \text{La}, \text{Sm}, \text{Nd}, \text{Yb}, \text{Lu}$) serve as effective, recyclable catalysts for the rapid intramolecular hydroalkoxylation (HO)/cyclization of primary/secondary and aliphatic/aromatic hydroxyalkenes in imidazolium-based room-temperature ionic liquids (RTILs) to yield the corresponding furan, pyran, spirobicyclic furan, spirobicyclic furan/pyran, benzo-furan, and isochroman derivatives. Products are straightforwardly isolated from the catalytic solution, conversions exhibit Markovnikov regioselectivity, and turnover frequencies are as high as 47 h^{-1} at 120°C . The ring-size rate dependence of the primary alkenol cyclizations is $5 > 6$, consistent with a sterically controlled transition state. The hydroalkoxylation/cyclization rates of terminal alkenols are slightly more

rapid than those of internal alkenols, which suggests modest steric demands in the cyclic transition state. Cyclization rates of aryl-functionalized hydroxyalkenes are more rapid than those of the linear alkenols, whereas five- and five/six-membered spirobicyclic skeletons are also regioselectively closed. In cyclization of primary, sterically encumbered alkenols, turnover-frequency dependence on metal-ionic radius decreases by approximately 80-fold on going from La^{3+} (1.160 Å) to Lu^{3+} (0.977 Å), presumably reflecting steric impediments along the reaction coordinate. The overall rate law for alkenol hydroalkoxylation/cyclization is

Keywords: alkenols • hydroalkoxylation • ionic liquids • lanthanide triflates • reaction mechanisms

$v \approx k[\text{catalyst}]^1[\text{alkenol}]^1$. An observed ROH/ROD kinetic isotope effect of 2.48 (9) is suggestive of a catalytic pathway that involves kinetically significant intramolecular proton transfer. The present activation parameters—enthalpy (ΔH^\ddagger) = 18.2 (9) kcal mol^{-1} , entropy (ΔS^\ddagger) = −17.0 (1.4) eu, and energy (E_a) = 18.2 (8) kcal mol^{-1} —suggest a highly organized transition state. Proton scavenging and coordinative probing results suggest that the lanthanide triflates are not simply precursors of free triflic acid. Based on the kinetic and mechanistic evidence, the proposed catalytic pathway invokes hydroxyl and olefin activation by the electron-deficient Ln^{3+} center, and intramolecular H^+ transfer, followed by alkoxide nucleophilic attack with ring closure.


Introduction

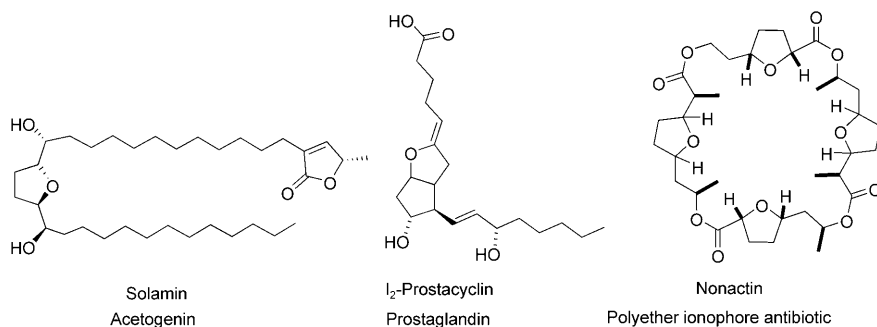
Catalytic regioselective O–H addition to the C=C bonds of pendant olefins is a highly desirable, atom-economical trans-

formation for accessing oxygen-containing heterocycles.^[1] Such heterocycles are important structural components of naturally occurring and biologically active molecules including acetogenins, prostaglandins, polyether ionophore antibiotics, and macrocyclic natural products.^[2] Currently, oxygen heterocycles are catalytically accessible by either direct Wacker oxidative cyclization^[3] or by means of intramolecular hydroalkoxylation (HO),^[4–7] with the latter being a relatively unexplored transformation mediated by a limited number of catalysts. In principle, intramolecular hydroalkoxylation is a concise, elegant route that should be possible to effect with 100% atom efficiency and with negligible waste coproduction. Thus, HO/cyclization fulfills green chemical requirements more satisfactorily than conventional byproduct-producing substitution reactions.^[1,8] However, although catalytic intramolecular hydroalkoxylation offers many at-

[a] Prof. T. J. Marks
Department of Chemistry and Material Science
Northwestern University
2145 Sheridan Road, Evanston IL 60208-3113 (USA)
Fax: (+1) 847-491-2990
E-mail: t-marks@northwestern.edu

[b] Dr. A. Dzudza
Department of Chemistry, Northwestern University
2145 Sheridan Road, Evanston IL 60208-3113 (USA)

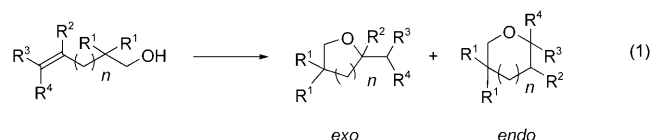
 Supporting information for this article, including experimental details and kinetic and mechanistic studies, is available on the WWW under <http://dx.doi.org/10.1002/chem.200902269>.



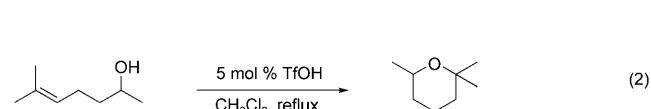
10 mol % [PdCl₂(MeCN)₂] affords β-alkoxyketones in high yield [Eq. (3)].

Subsequently, the Furukawa^[5f] and Oe^[5b,c] groups employed RuCl₃·*n*H₂O^[5f] and [(Cp**Ru*Cl₂)₂]^[5b,c] (Cp* = pentamethylcyclopentadienyl) catalysts to generate benzylic cyclic ethers by means of intramolecular HO [Eqs. (4) and (5)] in varying yields.

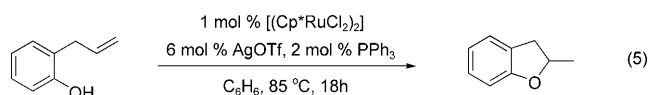
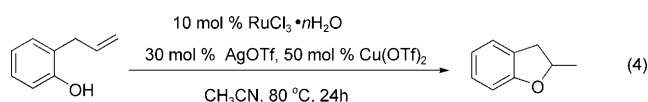
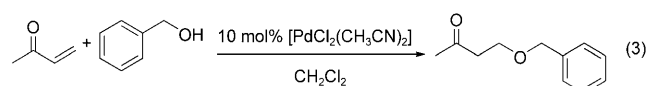
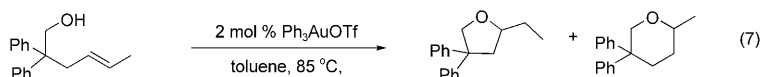
tractions, efficient transformations remain elusive due factors such as the large O–H bond enthalpies, the modest reactivity of electron-rich olefins with nucleophiles, high catalyst costs, and catalyst metal toxicity.^[5,6] There has been a growing research effort to address the aforementioned issues and to develop more efficient and selective hydroalkoxylation catalysts for this attractive transformation.^[4–7] For intramolecular alkenol HO/cyclizations, two possible products, exemplified by the *exo* and *endo* ethers shown in Equation (1), are a priori possible where either *exo*-trig or *endo*-trig cyclization to five- or six-membered rings is allowed by the Baldwin ring-closure rules.^[9]



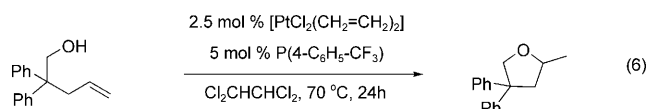
Although direct catalytic intramolecular OH addition to alkenes is attractive, such seemingly simple processes have not generally proven efficient and frequently lack generality. Catalysts have included Brønsted acids^[4] and transition-metal complexes,^[5,6] which activate either the hydroxyl or C=C double bond with varying degrees of efficiency. Duñach and co-workers employed catalytic amounts of triflic acid to generate Markovnikov-type cyclic ethers from unactivated olefins [Eq. (2)].^[4b]



However, several authors,^[5c,10] including Hartwig,^[4a] reported this approach to be of limited synthetic utility since controlling the acid concentration is crucial for acceptable yields. Of the effective intermolecular HO processes, transition-metal catalysis offers the potential to achieve selective olefin HO to Markovnikov products under mild conditions.^[5,6] The first example was reported by Murahashi and co-workers in 1989.^[12] Reaction of methyl vinyl ketones with BnOH in the presence of

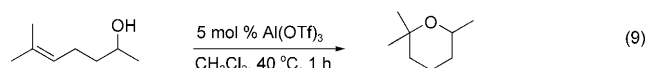
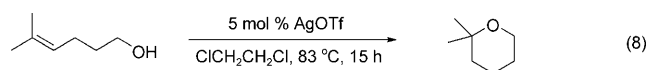


Moreover, RuCl₃·*n*H₂O catalytic activity is moderately enhanced by addition of AgOTf and Cu(OTf)₂ cocatalysts, thereby improving the yields without compromising selectivity.^[5f] In an example of Pt-catalyzed intramolecular HO/cyclization, Widenhofer et al. showed that [(PtCl₂(CH₂=CH₂))₂]/2 P(4-C₆H₄CF₃)₃ is an effective catalyst for cyclizing a range of γ- and δ-hydroxyolefins to yield highly substituted furans and pyrans [Eq. (6)].^[5d] The selectivity of the Pt system contrasts markedly with Pd-based catalysts, which tend to give oxidized products by means of Wacker-type oxypalladation/β-hydride elimination sequences.^[3]



Recently, He et al. made an important advance towards a general intermolecular hydroalkoxylation approach;^[5a] they reported that combining 2 mol % Ph₃PAuCl and 2 mol % AgOTf yields Ph₃PAuOTf, which in turn catalyzes a variety of hydroalkoxylation processes [Eq. (7)]; both *endo* and *exo* product formation is observed, with the latter formed in minor quantities.^[5a]

A variety of metal triflates have also been shown to effectively mediate intramolecular cyclization.^[6] For example, AgOTf, often used as a cocatalyst in Ru-catalyzed intramolecular HO/cyclizations of inert olefins, also mediates the transformation under relatively mild conditions [Eq. (8)].^[6d] Moreover, Duñach et al., in a combined experimental and theoretical study, showed Al(OTf)₃ to be an efficient catalyst for intramolecular cyclization of unactivated olefins [Eq. (9)].^[6b]



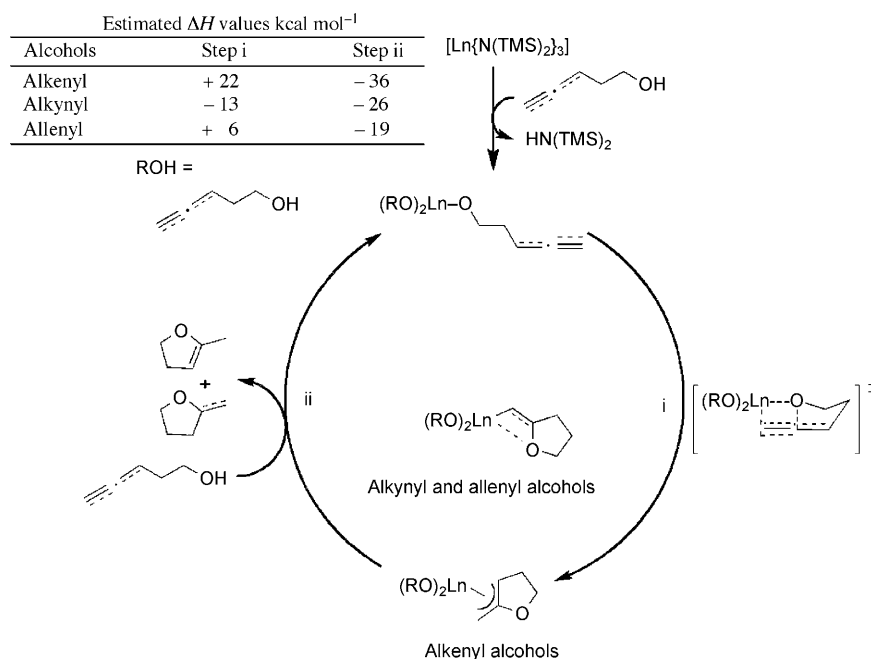
Nevertheless, due to the limitations of the current synthetic methodologies, for example, high catalyst cost,^[4,5] metal toxicity, and lack of catalyst recyclability, the development of new, more efficient catalysts and catalytic methods for cyclic ether synthesis presents an intriguing challenge.

Lanthanides exhibit a number of distinctive as well as potentially informative and useful characteristics for activating carbon–carbon unsaturation as well as amine, phosphine, and hydroxyl functionalities.^[7,12–16] Unique lanthanide-ion characteristics include high electrophilicity, very large ionic radii (which afford high coordination numbers and coordinative unsaturation), relatively constrained yet tunable ancillary ligation, and facile bond activation by means of concerted four-centered σ -bond metathesis processes, rather than by two-electron oxidative addition/reductive elimination sequences.^[12] Among these catalysts, homoleptic amides, for example, [Ln{N(SiMe₃)₂}]₃, and lanthanocenes, for example, [Cp*₂LnE(SiMe₃)₂], are versatile agents for a variety of C–C and C–heteroatom bond-forming transformations, which can be either intermolecular or intramolecular, and can exhibit very high turnover frequencies, versatile reaction scope in terms of heteroatom substitution pattern and ring size, as well as high stereoselectivity.^[7,13–15] Established catalytic transformations include, but are not limited to, polymerization processes,^[17] and hydroelementation processes such as

hydroamination,^[13] hydrophosphination,^[14] hydrosilation,^[15a] hydroboration,^[15b] and more recently, hydroalkoxylation.^[7] Moreover, hydroelementation can be coupled with catalytic polymerization, so that a variety of functional groups can be introduced into otherwise inert polyolefins.^[17a,b] Lastly, individual C–N and C–C bond-forming reactions can be tied in sequences to effect tandem processes.^[13a,b,16]

Recently, our group reported that homoleptic [Ln{N(SiMe₃)₂}]₃ complexes are effective and selective precatalysts for intramolecular HO/cyclization of alkynyl and allenyl alcohols.^[7] These precursors undergo instantaneous protonolysis at 25 °C to yield the corresponding alkoxides and free HN(SiMe₃)₂ (Scheme 1).^[7] Mechanistic data implicate turnover-limiting insertion of C–C unsaturation into the Ln–O bond (step *i*, Scheme 1) with subsequent, rapid Ln–C protonolysis (step *ii*, Scheme 1) to release product heterocycle and regenerate the catalyst.^[7] Although bonding energetic considerations^[18] predict net exothermic processes for all alcohols (see Scheme 1), the large Ln–O bond enthalpy^[18a,c] renders the insertive step *i* rather endothermic for alkenols, and likely for this reason, rapid intramolecular alkenol HO/cyclization has not yet been observed.^[7]

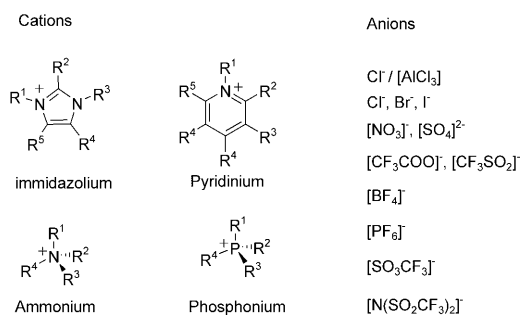
In the past decade, lanthanide triflates, [Ln(OTf)₃], environmentally friendly f-block element Lewis acids, have emerged as important reagents and catalysts.^[19–22] Kobayashi and co-workers popularized the application of lanthanide triflates as catalysts in Aldol reactions, Diels–Alder, retro- and aza-Diels–Alder reactions, allylation, and so on.^[19,20,22] Lanthanide ions have far larger ionic radii and formal coordination numbers than typical transition-metal ions,^[20a–c] and are very strong, hard Lewis acids. Nevertheless, lanthanide



Scheme 1. Proposed catalytic cycle for representative homoleptic lanthanide amido-catalyzed hydroalkoxylation/cyclization of alkyne- and allene-bearing alcohols (TMS = SiMe₃).

triflates are remarkably stable to hydrolysis,^[20a-c,21,22] and the strongly electron-withdrawing properties of the triflate counterion suggest an excellent leaving group.^[19,21b,22] In most cases, only substoichiometric (catalytic) quantities of $[\text{Ln}(\text{OTf})_3]$ effect useful catalytic turnover,^[19,21b,22] and they can be easily recovered on reaction completion and recycled with negligible loss of activity.^[19,21b,22] Nevertheless, conventional $[\text{Ln}(\text{OTf})_3]$ -catalyzed processes typically require toxic, polar, moderately coordinating solvents such as nitromethane and acetonitrile, which raise significant environmental and economic issues.^[23]

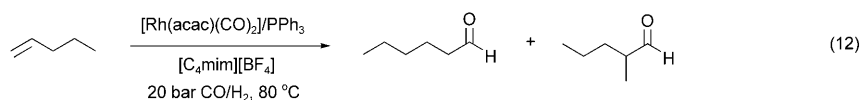
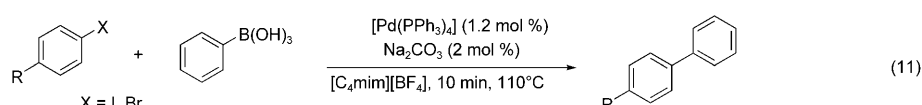
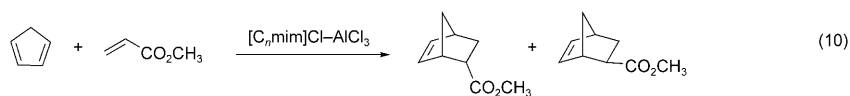
Ionic liquids (ILs) have generated increasing research interest as green alternatives to volatile organic solvents.^[24,25] They are comprised solely of positive and negatively charged ions,^[24,25] and typically have melting points below approximately 100 °C.^[24] Several types of ILs are free-flowing fluids at room temperature because large asymmetric constituent ions hinder close packing and thus lower the lattice energy.^[24] These are termed room-temperature ionic liquids (RTILs).^[24] IL physical and chemical properties depend on both the nature of the cation and anion,^[24] with typical organic cations being bulky, asymmetric imidazolium, pyridinium, ammonium, phosphonium, or other heteroaromatics, with low symmetry, weak intermolecular interactions, and delocalized/screened charge densities (Scheme 2).^[24] Popular



Scheme 2. Common ionic liquid cations and anions.

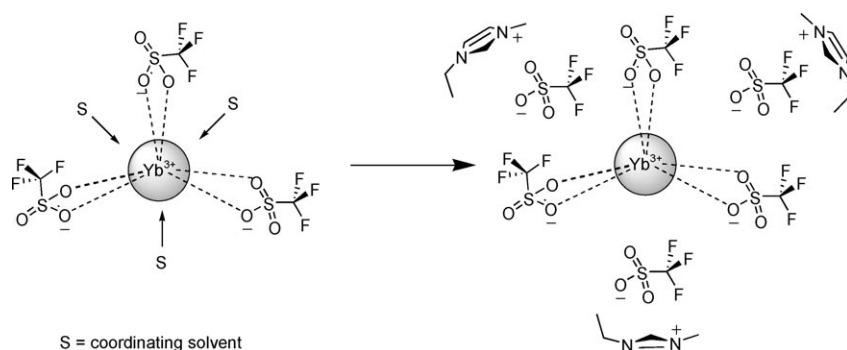
anions include Cl^- , Br^- , BF_4^- , PF_6^- , or CF_3SO_3^- , the properties of which, such as hydrogen-bond basicity, coordinative ability, and hydrophobicity, are readily manipulated (Scheme 2).^[24] In addition to high thermal stability and low volatility, ionic liquids have dielectric constants ranging from 10 to 28,^[26] are usually aprotic, and often afford unique reaction efficiencies and selectivities.^[24,25] Since IL properties such as miscibility with water and other solvents, solvation characteristics, polarity, viscosity, and density are tunable by anion and cation choice, they are considered to be “designer solvents.”^[24]

ILs are used in catalysis as the actual catalyst [Eq. (10)], as a ligand [Eq. (11)], or as the solvent [Eq. (12); acac = acetylacetonate].^[25–29] Chloroaluminate(III) ionic liquids, $[\text{C}_n\text{mim}]\text{Cl}-\text{AlCl}_3$ (C_nmim = 1-alkyl-3-methylimidazolium), are heavily exploited and well-studied IL catalysts,^[28] with Diels–Alder cycloaddition first demonstrated by Wolf et al.^[28d] Here rate enhancement effects are attributed to IL–polar substrate hydrogen-bonding.^[28d]



RTILs as ligands were first reported by Welton et al., who successfully performed Pd-catalyzed arene–arene Suzuki cross-coupling reactions in $[\text{C}_4\text{mim}][\text{BF}_4]$ [Eq. (11)].^[29a] Analysis of the solutions revealed the presence of a Pd phosphine-imidazolide complex.^[28b] The other major role played by ILs in catalytic processes is as the solvent.^[25,27,28] They have been exploited in hydrogenation by de Souza et al.^[30a] and Chauvin et al.,^[30b] hydroformylation by Song and Roh [Eq. (12)],^[30c] oxidation by Chauvin et al.,^[30b] Heck reactions by Kaufmann et al.,^[30d] and in many other processes.^[24,25] As solvents, ILs can provide better solvation by means of large dipolar and dispersion forces, and by means of hydrogen bonding.^[24,25,27] IL hydrogen-bond basicity is dominated by the anion, whereas hydrogen-bond acidity is dominated by the cation.^[24,25,27] Moreover, ILs with aromatic ions are capable of π – π and n – π interactions with solutes.^[24,25,27] In addition to the aforementioned attractions, ILs are thermally stable fluids, frequently allowing higher-reaction temperatures than conventional solvents, and ease of product separation by extraction or distillation.^[24,25,30] Proper IL choice can afford larger turnover frequencies, higher yields, and enhanced selectivity.^[30]

For $[\text{Ln}(\text{OTf})_3]$ -mediated intramolecular alkenol HO/cyclization, RTILs based on noncoordinating anions should enhance Ln^{3+} Lewis acidity due to minimized solvation (Scheme 3), and offer catalyst and IL recyclability, as well as ease of product separation by vacuum transfer or other extraction. In a recent communication, we briefly reported for a limited set of substrates, that in imidazolium-based ILs, $[\text{Ln}(\text{OTf})_3]$ -mediated alkenol HO/cyclizations are efficient processes for cyclic ether synthesis with Markovnikov selectivity.^[31] Herein we present a detailed report on the broad

Scheme 3. Enhancement of Ln^{3+} Lewis acidity due to minimization of solvent coordination.

reaction scope in terms of the ring size, substitution pattern, and selectivity of heterocycle formation, kinetics, and mechanism of $[\text{Ln}(\text{OTf})_3]$ -catalyzed intramolecular HO/cyclization of unactivated alkenols in RTILs. This full account includes discussion of reaction scope, selectivity, Ln ion effects, rate law, kinetic isotope effects, activation energetics, and proton-scavenging effects for this new catalytic process. In doing so, we compare the results with previously characterized Ln-mediated intramolecular hydroamination/cyclization and hydroalkoxylation/cyclization processes.

Results

The principal goal of this contribution is to examine the scope, selectivity, and mechanism of $[\text{Ln}(\text{OTf})_3]$ -mediated HO/cyclization of unactivated alkenols in imidazolium-based room-temperature ILs, to define the sequence of events that lead to the facile oxygen heterocycle formation. This section begins with observations concerning reaction-medium effects on the efficiency of the $[\text{Ln}(\text{OTf})_3]$ -catalyzed intramolecular HO/cyclization, followed by examination of the broad reaction scope in terms of the ring size, substitution pattern, and selectivity of heterocycle formation. Next, the dependence of reaction turnover frequency on Ln^{3+} ionic radius is discussed. Finally, a kinetic and mechanistic study of the HO/cyclization process includes examination of molecularity, activation parameters, OH/OD kinetic isotope effects, proton trapping, coordinative probing, and the mechanistic implications of these results.

Reaction-medium effects on catalytic alkenol HO/cyclization: The efficiency of the $[\text{Ln}(\text{OTf})_3]$ -catalyzed **1**→**2** conversion was first optimized as a function of solvent (Table 1), and an optimum reaction protocol was identified. Initial screening of $[\text{Ln}(\text{OTf})_3]$ -mediated intramolecular HO/cyclization of **1** in nitromethane revealed exclusive formation of **2** [Eq. (13)], Table 1]; the formation of β -hydride elimination/isomerization products was not observed. $[\text{Ln}(\text{OTf})_3]$ complexes exhibit modest catalytic activity for conversion **1**→**2** in nitromethane (Table 1, entries 1–3), with relative ordering of catalytic activity, $\text{Yb}^{3+} > \text{Sm}^{3+} > \text{La}^{3+}$. In marked contrast to the catalytic results in nitromethane, the

1→**2** catalytic conversion in RTILs based on weakly coordinating OTf^- and NTf_2^- anions proceeds with large rate enhancements, with approximately 70-fold increases in turnover frequencies (Table 1, entries 6–11). There is a general consensus that RTILs, in particular those based on imidazolium cations, have polarities comparable to those of short-chain alcohols and coordinative ten-

Table 1. Screening of $[\text{Ln}(\text{OTf})_3]$ complexes and reaction media for intramolecular hydroalkoxylation/cyclization of **1**.

Entry	$\text{Ln}(\text{OTf})_3$	Ln^{3+} [mol %]	M^{3+} [Å]	Solvent	$\epsilon^{\text{[a]}}$	N_t [h ⁻¹] (T [°C]) ^[c]
1	La	5	1.172	CD_3NO_2	36.4	0.01 (100) ^[d]
2	Sm	5	1.098	CD_3NO_2	36.4	0.04 (100) ^[d]
3	Yb	5	1.008	CD_3NO_2	36.4	0.10 (100) ^[d]
4	—	—	—	$[\text{C}_1\text{dbu}][\text{OTf}]^{\text{[e]}}$	^[b]	— (120)
5	—	—	—	$[\text{C}_2\text{mim}][\text{OTf}]^{\text{[f]}}$	15.1	— (120)
6	La	1	1.172	$[\text{C}_1\text{dbu}][\text{OTf}]^{\text{[e]}}$	^[b]	0.67 (120)
7	Yb	1	1.008	$[\text{C}_1\text{dbu}][\text{OTf}]^{\text{[e]}}$	^[b]	5.37 (120)
8	Yb	1	1.008	$[\text{C}_2\text{mim}][\text{OTf}]^{\text{[f]}}$	15.1	6.37 (120)
9	Yb	1	1.008	$[\text{C}_4\text{mim}][\text{OTf}]^{\text{[g]}}$	13.2	6.01 (120)
10	Yb	1	1.008	$[\text{C}_2\text{mim}][\text{NTf}_2]^{\text{[h]}}$	12.3	1.18 (120)
11	Yb	1	1.008	$[\text{C}_4\text{mim}][\text{NTf}_2]^{\text{[i]}}$	11.6	1.07 (120)

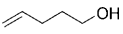
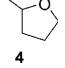
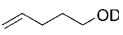
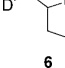
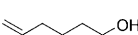
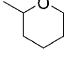

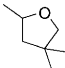
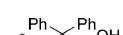
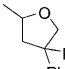
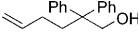
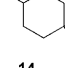
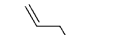
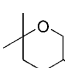
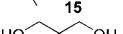
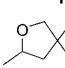
[a] Solvent dielectric constant at 25 °C. [b] Data not available in the literature. [c] Turnover frequencies determined by ^1H NMR spectroscopy using 1,1,2,2-tetrachloroethane as internal standard. [d] Percent formation of the final product was determined by ^1H NMR spectroscopy integration versus internal standard due to low observed product formation. [e] [1-Ethyl-3-methylimidazolium][OTf]. [f] [1-Methyl-1,3-diazabicyclo[5.4.0]undec-7-enium][OTf]. [g] [1-Butyl-3-methylimidazolium][OTf]. [h] [1-Ethyl-3-methylimidazolium trifluoromethanesulfonyl amide]. [i] [1-Ethyl-3-methylimidazolium trifluoromethanesulfonyl amide].

dencies similar to CH_2Cl_2 .^[24,25] Among these ILs, 1,3-dialkyl imidazolium RTIL derivatives based on OTf^- and NTf_2^- anions are minimally coordinating,^[24,25] thus likely enhancing Ln^{3+} Lewis acidity/unsaturation, in accord with the increased HO/cyclization turnover frequencies (Table 1, entries 6–9). The present large rate enhancements in the hydrophilic ionic liquid,^[25] $[\text{C}_n\text{mim}][\text{OTf}]$, versus the hydrophobic^[25] $[\text{C}_n\text{mim}][\text{NTf}_2]$ analogues (Table 1, entries 9 and 10), are reasonably attributable to solvation differences, with further explanation deferred to the Discussion section below.

Scope of catalytic alkenol intramolecular hydroalkoxylation/cyclization in $[\text{C}_2\text{mim}][\text{OTf}]$: To probe the scope of the present catalytic HO/cyclization process, a variety of substrates were examined with respect to regioselectivity, substituent effects, and turnover frequency. It can be seen that $[\text{Ln}(\text{OTf})_3]$ complexes in RTILs serve as effective catalysts for

the intramolecular (HO)/cyclization of primary/secondary and aliphatic/aromatic alkenols to yield the corresponding furan, pyran, spirobicyclic furan, spirobicyclic furan/pyran, benzofuran, and isochroman derivatives as summarized in Tables 2, 3, and 4, in which N_t is the turnover frequency at

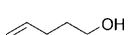
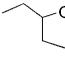
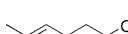
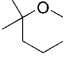
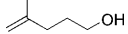
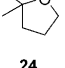

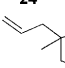
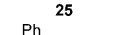
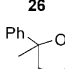
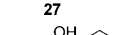
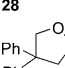

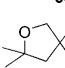

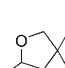
Table 2. $[\text{Ln}(\text{OTf})_3]$ -mediated hydroalkoxylation/cyclization of primary terminal alkenols in $[\text{C}_2\text{mim}][\text{OTf}]$.

Entry	Ln^{3+}	Substrate	Product	$N_t [\text{h}^{-1}]$ ($T [^\circ\text{C}]$) ^[a,b]
1	Yb			4.78 (120)
2	Sm	3	4	0.52 (120)
3	La			0.12 (120)
4	Yb			1.92 (120)
5	Yb	5	6	1.89 (120)
6	Sm			0.62 (120)
7	La	7	8	0.36 (120)
8	Yb			25.14 (120)
9	Sm	9	10	0.75 (120)
10	La			0.21 (120)
11	Yb			46.97 (120)
12	Sm	11	12	1.37 (120)
13	La			0.57 (120)
14	Yb			9.52 (120)
15	Sm	13	14	0.24 (120)
16	La			0.09 (120)
17	Yb			3.25 (60)
18	La	15	16	6.48 (60)
19	Yb			6.34 (120)
20	Sm	17	18	0.73 (120)
21	La			0.22 (120)

[a] Turnover frequencies determined by ^1H NMR spectroscopic integration versus internal standard. [b] For experimental details, see the Supporting Information.

the indicated temperature. In general, alkenol cyclizations proceed with near-quantitative conversions and reasonably large turnover frequencies at 1 mol % $[\text{Ln}(\text{OTf})_3]$ loading in 1–24 h at 60–120°C. In the present study, reaction progress is conveniently monitored by extracting the reaction aliquots of a known mass at preset times, recording the ^1H NMR spectrum, and monitoring intensity changes in the olefinic resonances, with $\text{Cl}_2\text{CHCHCl}_2$ used as the internal standard (see Figure 1). Turnover frequencies were determined from the slope of the kinetic plots of substrate: catalyst ratio versus time. The final furan, pyran, spirobicyclic furan, spirobicyclic furan/pyran, benzofuran, and isochroman products can be isolated either by simple ether extraction or by vacuum distillation. General workup conditions for preparative-scale reactions involve vacuum distillation of the volatiles from the ionic liquid and/or catalyst. In all cases, products were isolated and purified by flash chromatography, and characterized by ^1H , ^{13}C , and ^{19}F NMR spectroscopy,

Table 3. $[\text{Ln}(\text{OTf})_3]/[\text{C}_2\text{mim}][\text{OTf}]$ -mediated HO/cyclization of primary, sterically encumbered alkenols.

Entry	Ln^{3+}	Substrate	Product	$N_t [\text{h}^{-1}]$ ($T [^\circ\text{C}]$) ^[a,b]
1	Yb			0.023 (90)
2	Sm	19	20	0.019 (90)
3	La			0.012 (90)
4	Yb			0.19 (120)
5	Sm	21	22	0.31 (120)
6	La			1.63 (120)
7	Yb			7.88 (120)
8	Sm	23	24	0.36 (120)
9	La			0.11 (120)
10	Yb			5.15 (120)
11	Sm	25	26	0.64 (120)
12	La			0.31 (120)
13	Yb			14.89 (120)
14	Sm	27	28	1.74 (120)
15	La			0.49 (120)
16	Yb			30.15 (120)
17	Sm	29	30	1.22 (120)
18	La			0.48 (120)
19	Yb			8.62 (120)
20	Sm	31	32	1.04 (120)
21	La			0.29 (120)
22	Yb			7.61 (120)
23	Sm	33	34	0.85 (120)
24	La			0.19 (120)

[a] Turnover frequencies determined by ^1H NMR spectroscopic integration versus internal standard. [b] For more details, see the Supporting Information

and for new compounds, by high-resolution MS (HRMS) and/or elemental analysis (see the Experimental Section for details). Preparative-scale reactions were carried out in 50 mL three-neck round-bottomed flasks to afford isolated products in approximately 90% yield (see the Experimental Section for details).

$[\text{Ln}(\text{OTf})_3]$ -mediated HO/cyclizations of diverse alkenols in $[\text{C}_2\text{mim}][\text{OTf}]$ proceed with near-quantitative conversion and reasonably high turnover frequencies at 60–120°C (Tables 2, 3, and 4). Note that this process is effective in the catalytic formation of five- and six-membered mono- and bicyclic oxygen heterocycles. Note also that $[\text{Ln}(\text{OTf})_3]$ -catalyzed HO/cyclizations are not restricted to primary terminal and sterically encumbered hydroxyalkenes (Tables 2 and 3), and that secondary hydroxyalkenes also undergo cyclization (Table 4). This methodology is additionally applicable to aromatic hydroxyalkenes, as exemplified by synthesis of benzofurans and isochromans (Table 4). As illustrated in Tables 2–4), $[\text{Ln}(\text{OTf})_3]$ -catalyzed HO/cyclizations are effective for formation of diverse furans (Table 2, entries 1–4, 8–13; Table 3, entries 1–3, 7–9, 13–15; Table 4, entries 7–9, 13–15), pyrans (Table 2, entries 5–7, 14–18; Table 3, entries, 4–6; Table 4, entries, 10–12, 16–18), spirobicyclic furans (Table 2,

Table 4. $[\text{Ln}(\text{OTf})_3]$ -mediated HO/cyclization of secondary alkenols in $[\text{C}_2\text{mim}][\text{OTf}]$.

Entry	Ln^{3+}	Substrate	Product	N_t [h^{-1}] (T [$^{\circ}\text{C}$]) ^[a,b]
1	Yb			6.37 (120)
2	Sm			1.58 (120)
3	La			0.82 (120)
4	Yb			2.46 (120)
5	Sm			0.62 (120)
6	La			0.11 (120)
7	Yb			9.24 (120)
8	Sm			1.14 (120)
9	La			0.51 (120)
10	Yb			4.88 (120)
11	Sm			2.97 (120)
12	La			0.52 (120)
13	Yb			25.32 (90)
14	Sm			2.03 (90)
15	La			1.25 (90)
16	Yb			2.75 (120)
17	Sm			0.48 (120)
18	La			0.11 (120)

[a] Turnover frequencies determined by ^1H NMR spectroscopic integration versus an internal standard. [b] For more details, see the Supporting Information.

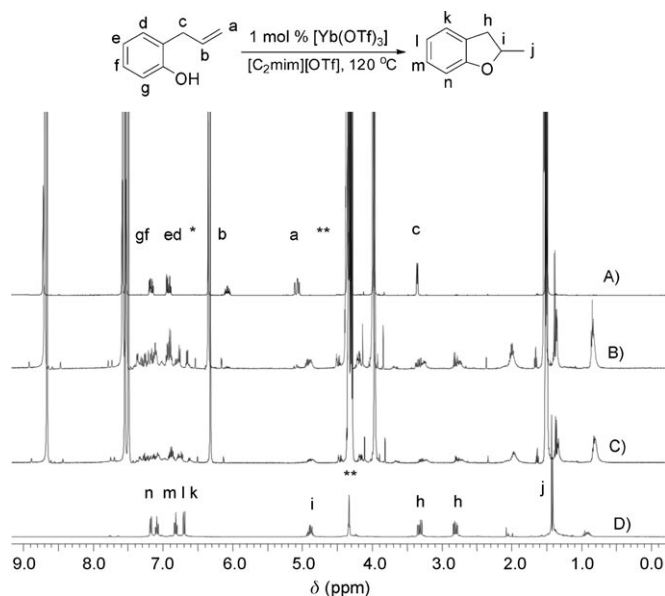


Figure 1. Typical ^1H NMR spectroscopy step plot of the $[\text{Yb}(\text{OTf})_3]$ -mediated $1 \rightarrow 2$ conversion in $[\text{C}_2\text{mim}][\text{OTf}]$. The reaction progress was monitored by extracting aliquots of a known mass at preset times and collecting the ^1H NMR spectrum (CD_3NO_2 , 500 MHz). Reaction conditions: $[\text{Yb}(\text{OTf})_3] = 1.0710 \times 10^{-2} \text{ M}$, $[1] = 1.07 \text{ M}$, $[1,1,2,2\text{-tetrachloroethane}] = 0.11212 \text{ M}$. A) $t = 0 \text{ min}$, B) $t = 5 \text{ min}$, C) $t = 10 \text{ min}$. D) ^1H NMR spectrum (CD_3NO_2 , 500 MHz) of clean final product **2** isolated by column chromatography (silica gel). [*] D_2O /Nitromethane. [**] 1,1,2,2-Tetrachloroethane. [***] Note: The aliquots varied slightly in the amounts of paramagnetic Yb^{3+} present, hence the slight discrepancies in ^1H chemical shifts.

entries 17 and 18; Table 3, entries 19–21), spirobicyclic furans/pyrans (Table 3, entries 16–18, 22–24), benzofuran (Table 4, entries 1–3), and isochroman (Table 4, entries 4–6). These are formed cleanly with the Markovnikov-type selectivity, also observed in Ru -,^[5c] Pt -,^[5d] Au -,^[5e] and Brønsted acid^[4b] based catalytic systems.

The ring-size dependence of $[\text{Ln}(\text{OTf})_3]/\text{RTIL}$ -catalyzed cyclization rates for the present primary and secondary hydroxyalkenes is $5 > 6$, which is consistent with a classical, sterically controlled ring-forming transition state (Table 2, entry 1 vs. 5, 11 vs. 14; Table 4, entry 13 vs. 16). For five-membered ring formation, the $3 \rightarrow 4$, $11 \rightarrow 12$, and $41 \rightarrow 42$ conversions ($N_t = 4.78$, 46.97, and 25.32 h^{-1} , respectively) are significantly more rapid than analogous six-membered molecules $13 \rightarrow 14$, $15 \rightarrow 16$, and $43 \rightarrow 44$ ($N_t = 1.89$, 9.52, and 2.75 h^{-1} , respectively), with N_t increasing by approximately three- to ten-fold. Interestingly, the ionic-radius-related N_t variations are markedly smaller than the approximately 10^3 -fold range observed in organolanthanide-mediated aminoalkene hydroamination/cyclization,^[13b,e] and larger than the approximately 20-fold effect range observed in organolanthanide-mediated hydroxyalkyne and hydroxyallene HO/cyclizations.^[7]

For substrates bearing geminal dimethyl and diphenyl substituents, significant rate enhancements are attributed to angle compression effects (“Thorpe–Ingold effect,” Table 2, entries 8–13, 20–22).^[13b,e,32] Thus, the $9 \rightarrow 10$ and $11 \rightarrow 12$ cyclizations proceed more rapidly than the analogous $3 \rightarrow 4$ ($N_t = 46.97 \text{ h}^{-1}$, and 25.14 vs. 4.78 h^{-1} , respectively) with N_t increased by approximately five- to ten-fold. The six-membered ring cyclizations of primary alkenyl alcohols **7** and **13** also exhibit a Thorpe–Ingold effect ($N_t = 1.89 \text{ h}^{-1}$ vs. 9.52 h^{-1} , respectively), but with diminished cyclization rates versus the five-membered rings. The same trend is observed in organolanthanide-mediated aminoalkene hydroamination^[13b,e] and hydroxyalkyne HO.^[7]

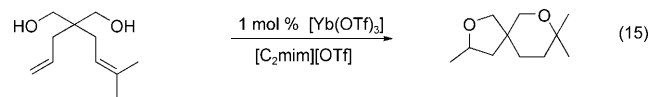
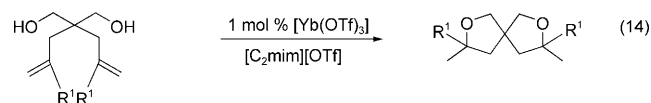
The catalytic sensitivity to olefin substituent steric encumbrance for conversions $15 \rightarrow 16$, $21 \rightarrow 22$, and $39 \rightarrow 40$ (Table 2, entries 17 and 18; Table 3, entries 4–6, 22–24; Table 4, entries 10–12) is generally consistent with the superiority of the larger ionic radius Ln^{3+} catalysts, reflected in a three-fold increase in N_t . This argues for a slightly sterically demanding transition state, thus reflecting subtle changes in the catalyst coordination environment.^[7] Interestingly, the $15 \rightarrow 16$, $21 \rightarrow 22$, and $39 \rightarrow 40$ cyclization regiochemistries are different from that expected from conventional Ln insertion/protonolysis catalytic processes^[7,13,14] (see more in the Discussion section). Furthermore, transformations $23 \rightarrow 24$ and $27 \rightarrow 28$ (Table 3, entries 7–9, 13–15) illustrate that cyclizations are not restricted to alkenols that bear substituents at terminal olefin positions. The present catalytic process is also applicable to alkenols that have substituents at internal olefinic positions (Table 3, entries 1–6, 16–18, 19–21). Note the $27 \rightarrow 28$ cyclization, which proceeds more rapidly than $23 \rightarrow 24$ ($N_t = 14.89$ vs. 7.88 h^{-1} respectively, at 120°C). If the transition state of this HO/cyclization process were partially or completely carbocationic, it would enjoy greater reso-

nance stabilization by phenyl over methyl substituents, as observed.

Note also that intramolecular hydroalkoxylation/cyclization of alkenol **25**, which bears a cyclopropyl substituent at the internal olefinic position, proceeds through cyclopropyl ring-opening to generate the furan **26** (Table 3, entries 10–12), thus plausibly supporting transient carbocationic species along the reaction coordinate (see more in the Discussion section).^[33]

Secondary alcohols results raise more intriguing questions about the structural effects that govern cyclization rates. HO/cyclization of aryl-functionalized secondary hydroxyalkenes proceeds at enhanced rates (Table 4, entries 1–6) versus linear hydroxyalkenes (Table 2, entries 1–3, 5–7), thereby suggesting some combination of Thorpe–Ingold/preorganization and electronic effects. For five-membered rings, the **1**→**2** transformation is slightly more rapid than **3**→**4** ($N_t = 6.37$ vs. 4.78 h^{-1} , respectively, at 120°C). For six-membered ring formation, the **7**→**8** versus **35**→**36** transformations experience similar acceleration magnitudes ($N_t = 2.75$ vs. 1.89 h^{-1} , respectively, at 120°C).

Another instructive observation here is that $[\text{Ln}(\text{OTf})_3]$ complexes also serve as efficient catalysts for the intramolecular HO/bicyclization of aliphatic dihydroxydienes to yield the corresponding bicyclic oxygen-containing frameworks as shown in Equations (14) and (15) (Table 2, entries 19–21; Table 3, entries 19–24).



These results demonstrate that C–O fusions can be regio-specifically coupled in sequence to exclusively assemble bicyclic rather than monocyclic products (Table 2, entries 17 and 18), especially rapid when smaller ionic radius $[\text{Yb}(\text{OTf})_3]$ is used. This catalytic transformation is therefore competent to form five/five and five/six polycyclic skeletons with a single catalyst center, and at turnover frequencies comparable to those of the corresponding primary and secondary hydroxyalkene cyclizations (**3**, **21**, and **23**, respectively) for the same catalyst, temperatures, and reaction conditions (Table 2, entry 1; Table 3, entries 4 and 7).

Metal ion effects on catalytic alkenol hydroalkoxylation/cyclization: For the representative cyclization **11**→**12** [Eq. (16)], Table 5 shows that N_t increases substantially with a decrease in the Ln ionic radius. Proceeding from the largest eight-coordinate ionic radius, La^{3+} (1.160 \AA),^[34] to intermediate Sm^{3+} (1.079 \AA), to the smallest six-coordinate ionic radius, Lu^{3+} (0.977 \AA),^[34] the N_t variation spans a rate factor

Table 5. The effect of varying Ln^{3+} ionic radius on catalytic intramolecular HO/cyclization turnover frequency.

Entry	Ln^{3+}	Ionic radius	$N_t [\text{h}^{-1}] (T [^\circ\text{C}])^{[a,b]}$
1	La	1.160	0.57 (120)
2	Nd	1.109	1.21 (120)
3	Sm	1.079	1.37 (120)
4	Yb	1.008	46.97 (120)
5	Lu	0.977	47.15 (120)

[a] Turnover frequencies measured in $[\text{C}_2\text{mim}][\text{OTf}]$ with 1 mol % catalyst. [b] For details, see the Supporting Information.

of over approximately 80-fold, with HO/cyclization more rapid for smaller ionic radius catalysts. The effects of Ln^{3+} ionic radius on the aliphatic/aromatic alkenol cyclization N_t values generally parallel Ln contraction trends^[19] (Table 5), with the smallest, most Lewis acidic^[20a–c] Ln^{3+} center in most cases being more efficient. This pattern parallels that of organolanthanide-catalyzed aminoalkyne hydroamination/cyclization,^[13a,f] but not that of aminoalkenes^[13b,e] or of hydroxyalkynes and hydroxyallenes.^[7] Further explanations are deferred to the Discussion section.

Kinetic and mechanistic studies: Most kinetic data acquired in this study were obtained using the $[\text{Yb}(\text{OTf})_3]$ catalyst. The rationale is two-fold: 1) the small ionic radius leads to increased cyclization rates, thus increasing efficiency and accuracy in measurements on less reactive substrates, 2) the relatively short Yb^{3+} T_{1e} (electron spin-lattice relaxation time) allows convenient and informative NMR spectroscopic monitoring of reactions without excessive line broadening induced by some other paramagnetic Ln ions. Quantitative kinetic studies of representative cyclization **1**→**2** were carried out in the presence of 1–10 mol % $[\text{Yb}(\text{OTf})_3]$ catalyst in $[\text{C}_2\text{mim}][\text{OTf}]$. Kinetics were monitored from intensity changes in the substrate olefinic resonances over three or more half-lives. The concentration of product **2** was measured from the area of the olefinic resonances (Figure 1) standardized to the area of the CH_2 peak of added 1,1,2,2-tetrachloroethane. The methylene signal of 1,1,2,2-tetrachloroethane ($\delta = 6.26 \text{ ppm}$) can be readily distinguished from substrate **1** and product **2** resonances at 500 MHz. These cyclizations were performed with a 100-fold molar excess of substrate over the catalyst, and NMR spectroscopic analysis indicates that, within the instrumental limits, only substrate and product are present in detectable quantities at all stages of conversion. Monitoring substrate consumption as a function of time (Figure 2A) yields initial rate constants (Figure 2B).

A van 't Hoff plot of $\ln k_{\text{obs}}$ versus $\ln [\mathbf{1}]$ reveals a linear relationship consistent with a first-order dependence in the concentration of **1** (Figure 2C). The same trend is observed for the k_{obs} dependence on the $[\text{Yb}(\text{OTf})_3]$ concentration (Figure 2D). Kinetic studies under the same conditions but at different substrate **1** and $[\text{Yb}(\text{OTf})_3]$ catalyst concentra-

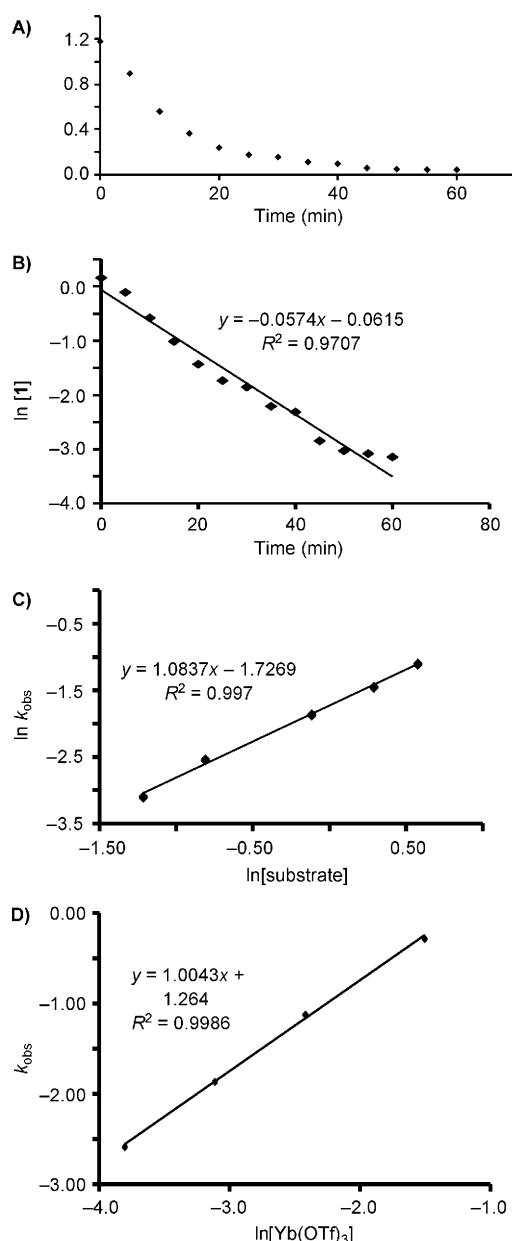


Figure 2. A) Concentration of starting material (**1**) as a function of time for the hydroalkoxylation/cyclization using $[\text{Yb}(\text{OTf})_3]$ as the catalyst in $[\text{C}_2\text{mim}][\text{OTf}]$ at 120°C . B) Determination of k_{obs} from the plot of $\ln[1]$ versus time. C) van't Hoff plot of the hydroalkoxylation/cyclization of **1** using $[\text{Yb}(\text{OTf})_3]$ as the catalyst in $[\text{C}_2\text{mim}][\text{OTf}]$ at 120°C . The lines are least-squares fits to data points. D) van't Hoff plot of the hydroalkoxylation/cyclization of **1** using $[\text{Yb}(\text{OTf})_3]$ as the catalyst in $[\text{C}_2\text{mim}][\text{OTf}]$ at 120°C . The lines are least-squares fits to data points.

tions yield linear plots of rate versus substrate concentration. By combining these results, the overall experimental rate law can be expressed as in Equation (17). The **1**→**2** $[\text{Yb}(\text{OTf})_3]$ -mediated intramolecular HO/cyclization rate law is overall second-order, but first-order in substrate and catalyst.

$$v \approx k[\text{Yb}^{3+}]^1[\mathbf{1}]^1 \quad (17)$$

Turnover frequencies, N_t (h^{-1}), were calculated from the least-squares determined slope (m) according to Equation (21) (see the Experimental Section for details). Determination of the cyclization N_t values for other substrates was carried out in the same way as for the cyclization **1**→**2**. Standard Eyring (Figure 3B) and Arrhenius (Figure 3C)

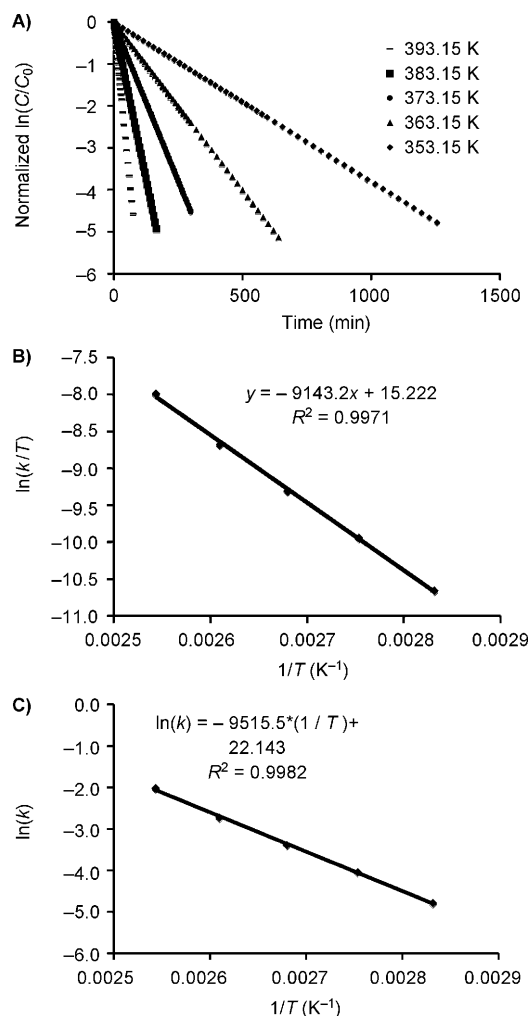


Figure 3. A) Natural log of product **3** concentration as a function of time and temperature for the hydroalkoxylation/cyclization of **3** using 1 mol % of $[\text{Yb}(\text{OTf})_3]$ catalyst in $[\text{C}_2\text{mim}][\text{OTf}]$ at various temperatures. B) Eyring plot for the intramolecular hydroalkoxylation/cyclization of **3** using $[\text{Yb}(\text{OTf})_3]$ catalyst in $[\text{C}_2\text{mim}][\text{OTf}]$. The lines represent the least-squares fit to the data points. C) Arrhenius plot for the intramolecular hydroalkoxylation/cyclization of **3** using $[\text{Yb}(\text{OTf})_3]$ catalyst in $[\text{C}_2\text{mim}][\text{OTf}]$. The lines represent the least-squares fit to the data points.

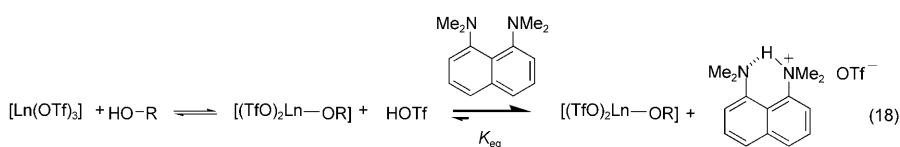
analyses^[35] of data obtained in variable-temperature experiments yielded enthalpy (ΔH^\ddagger) = 18.2 (9) kcal mol^{-1} , entropy (ΔS^\ddagger) = -17.0 (1.4) eu, and energy (E_a) = 18.9 (8) kcal mol^{-1} activation parameters.^[36] The errors in these parameters were computed from published error propagation formulas,^[35b] which were derived from the Eyring equation^[35] using the OriginPro 7.5 program.

Kinetic isotope effect data (-OH versus -OD) were acquired for the cyclization **5**→**6** (Table 2, entries 1 and 4) by

^1H NMR spectroscopy, and yield $k_{\text{H}}/k_{\text{D}}=2.48$ (9), which is suggestive of a primary kinetic isotope effect. The ^2H NMR spectrum of cyclized product **6** shows it to be monodeuterated at the 2-methyl position (see the Supporting Information). Proton-transfer processes typically exhibit KIEs of 2.5–7.0.^[37] Although NH/ND labeling studies for analogous organolanthanide-catalyzed alkene hydroamination processes also exhibit a primary KIE with same ^2H regioselectivity,^[13b] a number of pathways that yield the same regioselectivity can be envisioned for H^+ transfer in the present case, for example, olefin insertion into the $\text{Ln}-\text{O}$ bond followed by inter/intramolecular proton transfer, or Ln^{3+} -coordinated alkoxide nucleophilic attack on olefin, with pre-/post- inter-/intramolecular proton transfer (see the Discussion Section).

Mechanistic investigations with proton-trapping reagents:

The pathways for hydroalkoxylation/cyclization catalyzed by TfOH and main-group metal triflates are proposed to be closely related,^[4a] since the reaction selectivities are similar.^[4a,5a] In principle, $[\text{Ln}(\text{OTf})_3]$ complexes could serve as a source of a protic acid such as TfOH, a known catalyst for intramolecular hydroalkoxylation/cyclization of unactivated alkenes.^[4b] A classic test for proton-transfer participation involves monitoring the reaction rate in the presence of sterically hindered amine “proton sponges,” for example, 2,6-di-*tert*-butylpyridine (DTP) or *N,N,N',N'*-tetramethyl-1,8-naphthalenediamine (TMAN), which differ in their basicities ($\text{p}K_{\text{a}}=3.6$ and 12.1, respectively).^[38,39a,d] In the case of Brønsted acid catalysis, the H^+ is captured by the base, thereby resulting in a depression or suppression of the cyclization rate [Eq. (18)].^[38,39]



For the present comparative studies of $[\text{Ln}(\text{OTf})_3]$ - and TfOH-catalyzed (1 and 3 mol %, respectively) **1**→**2** HO/cyclization, the two proton sponges employed exhibit different inhibition patterns. Kinetic results for $[\text{Yb}(\text{OTf})_3]$ - and TfOH-mediated cyclizations reveal that the former turns over approximately seven-fold faster (Figure 4), and that the two proton sponges affect the respective reaction rates differently. For $[\text{Yb}(\text{OTf})_3]$ -mediated **1**→**2** cyclization, low TMAN concentrations marginally affect the N_{t} values; only upon the addition of three equivalents of TMAN is cyclization completely inhibited (Figure 4). In contrast, 2,6-di-*tert*-butylpyridine addition (1.0 equiv) to the $[\text{Yb}(\text{OTf})_3]$ catalytic mixture results in complete inhibition of turnover (Figure 4). For TfOH-mediated **1**→**2** HO/cyclization, incremental TMAN addition (0.5–3.0 equiv) decreases the rate in an approximately linear fashion (Figure 4). Thus, the trapping experiments that utilize TMAN and DTP indicate that proton sponges affect $[\text{Yb}(\text{OTf})_3]$ - and TfOH-mediated cyc-

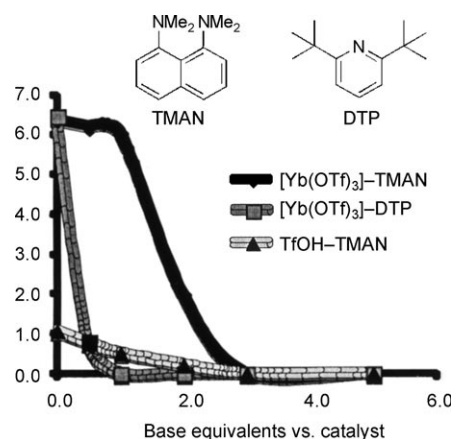


Figure 4. The effect of varying concentration of sterically hindered base on $[\text{Yb}(\text{OTf})_3]$ - and TfOH-mediated **1**→**2** cyclization in $[\text{C}_2\text{mim}][\text{OTf}]$. For experimental details, see the Supporting Information. Lines through data points are drawn to guide the eye.

lization rates differently, the explanation of which is deferred to the Discussion section.

^{19}F NMR spectroscopic analysis of the $[\text{Yb}(\text{OTf})_3]$ - and TfOH-mediated **1**→**2** HO/cyclization reaction mixture volatiles, trapped by vacuum transfer after 15 min reaction, confirm the presence of triflic acid ($\delta = -77.14$ ppm) only in the case of the TfOH-mediated reaction (see the Experimental Section). These results argue that lanthanide triflates do not serve as free TfOH precursors, even though the proton-trapping results suggest the involvement of protons in the catalytic cycle. These results imply that other possible alkenol deprotonation pathways may be responsible for the catalyst deactivation and observed decrease in cyclization turnover frequencies.

To better understand the origin of the acidic proton trapped in the proton sponge experiments, additional proton traps that have different properties were explored. Of particular interest were non-nucleophilic traps that react rapidly and irreversibly with protons. Here, main group aryls of the type $\text{R}_n\text{E}-\text{Ar}$, for example, $\text{R}_3\text{-Sn-Ph}$ and $\text{R}_3\text{-Si-Ph}$, are attractive candidates since they exhibit substantial $\text{E}-\text{aryl}$ cleavage rates in the presence of protons to yield readily identifiable arenes and the corresponding $\text{E}-\text{OTf}$ species.^[38,40] Therefore, $[\text{Yb}(\text{OTf})_3]$ -mediated **3**→**4** cyclization was carried out in the presence of Me_3SiPh (1.0 equiv per $[\text{Yb}(\text{OTf})_3]$) in $[\text{C}_2\text{mim}][\text{OTf}]$. The reaction produces only small quantities of HO/cyclization product ($\approx 2\%$ yield) along with benzene (5 mol %) and Me_3SiOTf (5 mol %), as indicated by ^1H and ^{19}F NMR spectroscopic analysis of the reaction mixture. Furthermore, a stoichiometric mixture of Me_3SiPh and **3** remains unchanged after 12 h under identical reaction conditions. These results argue that H^+ scavenging by Me_3SiPh inhibits HO/cyclization and deactivates the catalyst stoichiometrically. These results implicate the requirement of the Ln^{3+} catalyst in facili-

tating a proton transfer, which does not appear to originate from free triflic acid, but rather from the alkenol hydroxyl group. Literature reports also indicate that metal triflates do not readily eliminate HOTf in the presence of alcoholic nucleophiles.^[41]

Coordinative probing of the Yb³⁺-olefin interaction: While kinetic studies provide the overall reaction molecularity and suggest the turnover-limiting step, in situ ¹H NMR spectroscopic experiments give qualitative insight into which substrate and product species enter the paramagnetic Ln³⁺ coordination sphere. In the present study, arrayed ¹H NMR spectroscopic experiments were carried out over the course of the [Yb(OTf)₃]-mediated **15**→**16** HO/cyclization, which probed Yb³⁺-olefin/alcohol interactions by means of chemical-shift changes of the olefinic and methylene (adjacent to -OH) ¹H resonances. Yb³⁺ was chosen, since it induces isotropic paramagnetic shifts accompanied by reasonably small line broadening. In [Yb(OTf)₃]-mediated **15**→**16** HO/cyclization, substantial upfield shifts of the olefinic and methylene (adjacent to -OH) proton resonances are observed on initiation and during the course of turnover [Eq. (19) and Figure 5].

$$N_t = \frac{m}{[\text{catalyst}]_0} \quad (19)$$

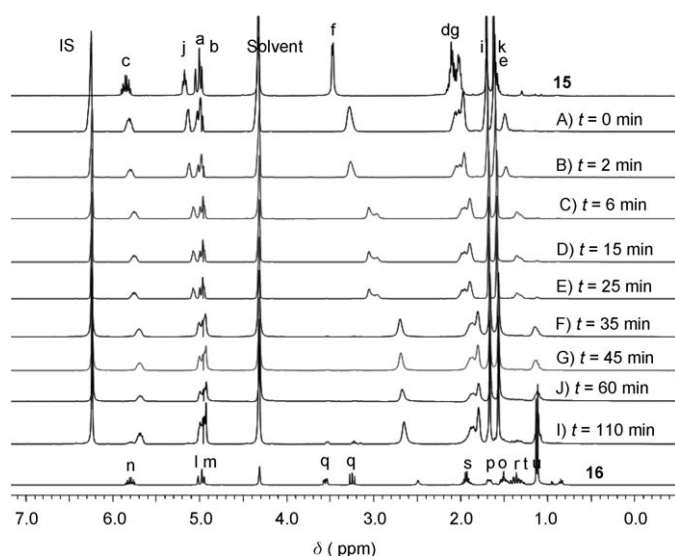


Figure 5. Overlaid 500 MHz ¹H NMR spectra of the [Yb(OTf)₃]-mediated **15**→**16** cyclization reaction solution, in [D₃]nitromethane at room temperature. For more details, see the Experimental Section.

Discussion

Reaction-medium effects on the catalytic alkenol hydroalkoxylation/cyclization process: Derivatives of 1,3-dialkylimidazolium cations associated with a variety of anions are among the most widely used and investigated classes of

RTILs, primarily because of the possibility of fine-tuning of the physicochemical properties through the *N*-alkyl substituents and anions. Imidazolium-based ionic liquids display pronounced self-organization in the solid and liquid phases, an extended network of cations and anions interconnected by hydrogen bonds.^[24,25] Introduction of solute disrupts the extended network, thereby allowing the IL to act as a hydrogen-bond donor (cation) or acceptor (anion), thus interacting with substrates that have accepting and donating sites, respectively. The Hughes–Ingold rules, which describe solvent effects on reaction rates, are essentially qualitative and rely on generalized solvent polarity concepts.^[42] For molecular solvents, polarities are commonly expressed in terms of the dielectric constant, thus implying an electrostatic solvation model. Much effort has been made to develop empirical solvent-polarity scales for RTILs to aid in explaining/predicting differences in solvation effects.^[26] For most RTILs, the single-parameter polarity approach has not been definitive because most RTILs appear to fall within the same narrow range of values.^[26] Yet, as shown here, two different ionic liquids that have essentially the same polarity indices produce significantly different results as solvents for HO/cyclization. Clearly, a single polarity parameter is insufficient to describe the variations in experimental results.

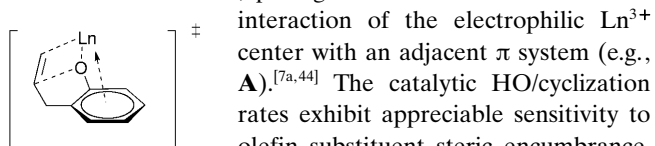
In comparison to unimolecular solvents, which have a limited number and type of interactions with solutes, ionic liquids, given their diverse structures and functionality, are complex and capable of many types of solvating interactions (e.g., dispersive, π - π , n - π , hydrogen-bonding, dipolar, ionic, charge-charge), with many of these interactions occurring simultaneously, thereby enhancing solvation and reaction efficiencies.^[24–26,43] Due to the inherent polarity of RTILs, reactions that involve charge development in the transition state will likely experience greater transition-state stabilization than in polar unimolecular solvents.^[43] Identifying the types of solute-solvent interactions between RTILs and substrates is useful in explaining the origin of rate enhancements, which can depend upon both RTIL constituents.^[43] Solvation studies based on linear free-energy approaches to analyze RTIL interactions with probe solute molecules reveal that [C₆mim][OTf] exhibits greater hydrogen-bond basicity than does the NTf₂⁻ analogue, thus producing stronger interactions with solutes such as alkenols, and resulting in rate accelerations for polar transition states.^[43]

Scope of catalytic intramolecular hydroalkoxylation/cyclization

A central goal of this investigation was to explore the scope of [Ln(OTf)₃]-mediated intramolecular cyclization of terminal/internal primary and secondary aliphatic/aromatic alkenols. The results in Tables 2–4 indicate that [Ln(OTf)₃] complexes are competent catalysts for the formation of diverse five- and six-membered oxygen heterocycles that have a wide variety of alkyl and aryl substituents. The ring-size dependence of [Ln(OTf)₃]/RTIL-catalyzed cyclization rates for the primary alkenols is 5 > 6, which is consistent with a classical, sterically controlled ring-forming transition state (Table 2, entry 2 vs. 5, entry 6 vs. 8).^[13–15] In general, the

five-membered ring transformations proceed more rapidly than the analogous six-membered rings, with N_t increasing by approximately three- to ten-fold. The same trend is observed in organolanthanide-mediated hydroaminations, but with far larger rate dispersions than observed here.^[13]

In the HO/cyclizations of both primary and secondary alkenols, there are distinct differences in rates between alkyl and aromatic substrates. In general, cyclization rates of aryl-functionalized alkenols are slightly more rapid than those of the linear hydroxyalkenes. This may reflect transition-state configurations in which the aryl-functionalized substrates have more accessible, preorganized structures that involve



interaction of the electrophilic Ln^{3+} center with an adjacent π system (e.g., **A**).^[7a,44] The catalytic HO/cyclization rates exhibit appreciable sensitivity to olefin substituent steric encumbrance.

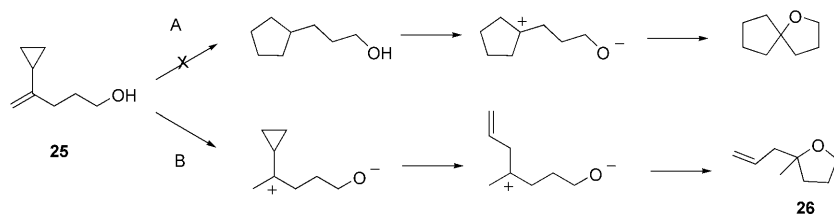
In general, terminal alkenol cyclization rates (Table 2) are greater than those of sterically encumbered alkenols (Tables 3 and 4). For alkenols that bear two substituents at the olefin terminus, the superiority of the larger ionic radius Ln^{3+} catalysts is evident, as reflected in an approximately nine-fold N_t increase. R substituent effects on cyclization rates can be rationalized to some degree in terms of a slightly sterically demanding transition state in which the R substituent occupies a less encumbered position, thus reflecting subtle changes in the catalyst coordination environment.^[13,45] Moreover, the regiochemistry of the **15**→**16**, **21**→**22**, and **39**→**40** cyclizations is different from what is expected in conventional lanthanide C=C insertion/protonolysis sequences,^[7,13–15] thereby suggesting a pathway in which the Ln^{3+} center facilitates intramolecular proton transfer, followed by alkoxide nucleophilic attack (see more below).

Intramolecular HO/cyclization of alkenol **25**, which bears a cyclopropyl substituent at the internal olefinic position, provides information on the nature of transient species along the reaction coordinate. Cyclopropyl substituents are highly strained and suffer both Bayer (angular)^[33a] and Pitzer (torsional) strain,^[33a] thereby resulting in pronounced reactivity.^[33] Possible rearrangement routes for HO/cyclization are illustrated in Scheme 4 and take into account the established, greatly altered reactivity when in conjugation with an adjacent π system.^[33] In route A (Scheme 4), the process traverses a well-documented, thermally induced vinylcyclopropane unimolecular rearrangement pathway to yield a cyclopentene, for which a concerted pathway has been proposed.^[46] If the first step is thermally induced rear-

rangement, followed by intramolecular H^+ transfer and alkoxide nucleophilic attack (or conventional HO/cyclization^[7]), the cyclization would presumably result in a spirofuran (Scheme 4, route A). Alternative pathway B (Scheme 4), in which H^+ transfer results in cyclopropyl ring opening, involves a transitory allylcarbynyl cation, which when quenched by an alkoxide nucleophile would result in **26**, the observed final product, and consistent with cyclopropyl rearrangement route B. Prior studies have shown that main group triflate-mediated methylenecyclopropane ring opening with alcoholic nucleophiles proceed along route B (Scheme 4).^[41]

Regarding 1,3-diol-alkenyl substrates, the present $[\text{Yb}(\text{OTf})_3]$ -mediated intramolecular HO/bicyclization coupling process is capable of regiospecific closing of five- and five/six-membered spirobicyclic skeletons [Eqs. (14) and (15)]. These results (Tables 2 and 3) illustrate that two C–O bond fusions can be coupled in sequence at a single Ln^{3+} center to exclusively assemble bicyclic products. The substrates that were examined form Markovnikov-regiospecific spirobicyclic furans/pyrans. The increased N_t for the $[\text{Yb}(\text{OTf})_3]$ - versus $[\text{La}(\text{OTf})_3]$ -mediated HO/cyclization of **33**→**34** versus that of parent molecule **15** suggests that the interplay of factors including sterics, electronics, and metal-coordination strength govern the rates.

Metal-ion effects: Catalytic activity dependence on metal-ion size has previously been observed in other Ln^{3+} -mediated transformations.^[7,13,14] In the present study, N_t variation spans a factor of over approximately 80-fold from the largest eight-coordinate ionic radius, La^{3+} (1.160 Å),^[34] to intermediate Sm^{3+} (1.079 Å),^[34] to the smallest six-coordinate ionic radius, Lu^{3+} (0.977 Å)^[34] (Table 5). Interestingly, the present range of N_t variations is markedly smaller than the approximately 10^3 -fold range observed in organolanthanide-mediated aminoalkene hydroamination/cyclization,^[13e] but larger than the approximately 20-fold range observed in organolanthanide-mediated hydroxyalkyne and hydroxyallene HO/cyclizations,^[7] presumably reflecting significant steric and electronic differences along the different reaction coordinates.^[13e,45] In the present study, the HO/cyclization rates of alkenols that bear two substituents at the olefin terminus follow an opposite trend to cyclization rates of terminal alkenols, with larger radius lanthanides correlating with greater reaction rates. In the latter case, the observed behavior is most likely due to steric hindrance of olefin approach and activation by the catalytic center.^[13e,45]



Scheme 4. Plausible **25**→**26** rearrangement hydroalkoxylation/cyclization routes A and B.

Kinetics and mechanism of intramolecular alkenol hydroalkoxylation/cyclization: The kinetic results for the **1**→**2** conversion were acquired by using $[\text{Yb}(\text{OTf})_3]$, and yield the empirical rate law $v \approx k[\text{catalyst}]^1[\text{substrate}]^1$. This first-order dependence on sub-

strate is significantly different from the zero-order dependence observed in homoleptic lanthanide amido- or lanthanocene-mediated hydroamination/cyclization and HO/cyclization processes.^[7,13] The observed zero-order (substrate) dependence argues for turnover-limiting intramolecular olefin insertion into an Ln–N/Ln–O bond (Scheme 1),^[7,13] in accord with thermodynamic considerations^[17] and DFT-level quantum chemical calculations.^[45] The rate law in the present case argues that either alkenol complexation is turnover-limiting (step *i*, Scheme 5), or that proton transfer (step *ii*, Scheme 5) following a rapid pre-equilibrium is turnover-limiting (hence the observed kinetic isotope effect; see below). Following subsequent alkoxide nucleophilic attack/ring closure (step *iii*, Scheme 5), product dissociation

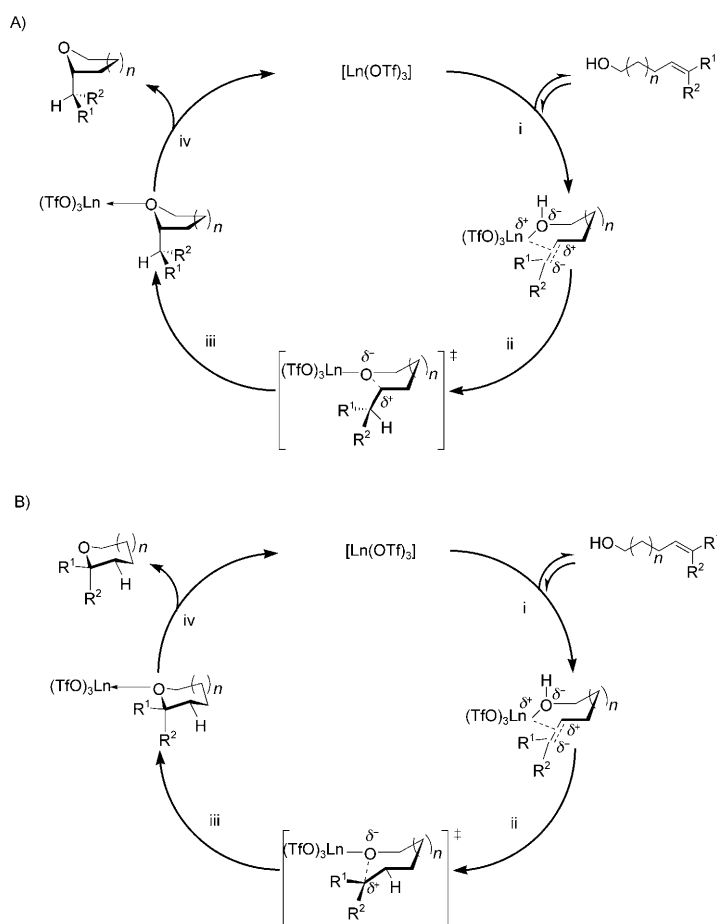
Table 6. Kinetic isotope effects comparison observed for intramolecular hydroamination/cyclizations and intramolecular hydroalkoxylation/cyclizations processes.

Entry	Catalyst	Substrate	Product(s)	k_H/k_D
1 ^[a]	[Yb(OTf) ₃]			OH/OD = 2.48 (9)
2 ^[b]	[La{N(SiMe ₃) ₂ }] ₃			OH/OD = 0.95 (3)
3 ^[c]	[Cp* ₂ LaN(SiMe ₃) ₂]			NH/ND = 2.7 (4)
4 ^[c]	[Cp* ₂ LaN(SiMe ₃) ₂]			NH/ND = 5.2 (8)

[a] Determined using the catalyst in [C₂mim][OTf]. [b] Determined using the precatalyst in [D₆]benzene.^[7] [c] Determined using the precatalyst in [D₈]toluene.^[13b]

(step *iv*, Scheme 5) regenerates the [Ln(OTf)₃] catalyst. Kinetic isotope effect (KIE) data (–OH vs. –OD) for cyclizations **3**→**4** and **5**→**6** (Table 2, entries 1 and 4) yield k_H/k_D = 2.48 (9) (Table 6, entry 1). This value is consistent with proton-transfer processes, which usually exhibit primary KIEs of 2.5–7.0,^[37] and that it is part of the turnover-limiting step or is intimately coupled to it. The magnitude of this KIE is reminiscent of values observed for organolanthanide-catalyzed aminoalkene hydroamination process,^[13b] but stands in contrast to a nonprimary effect observed for homoleptic lanthanide amido-catalyzed hydroxyalkyne and hydroxyallene hydroalkoxylation processes,^[7] as summarized in Table 6. Moreover, ²H NMR spectra of cyclized product **6** show it to be monodeuterated at the 2-methyl position. Note that NH/ND labeling studies for the analogous organolanthanide-catalyzed aminoalkene hydroamination processes also exhibit primary KIEs with the same deuterium regioselectivity,^[13b] however, experimental and theoretical evidence here for turnover-limiting olefin insertion into Ln–N is compelling.^[13]

Variable-temperature kinetic studies of the **3**→**4** hydroalkoxylation/cyclization yield activation parameters ΔH^\ddagger = 18.2 (9) kcal mol^{–1}, ΔS^\ddagger = –17.0 (1.4) eu, and E_a = 18.9 (8) kcal mol^{–1} (Table 7, entry 7). Organolanthanide-mediated intramolecular hydroamination and HO processes (Table 7, entries 1–6) proceed with moderate activation enthalpies and energies, but with negative ΔS^\ddagger values, thereby suggesting highly organized transition states. The somewhat higher ΔH^\ddagger and E_a values and a negative ΔS^\ddagger value^[7] observed for intramolecular HO/cyclization (Table 7, entry 6) most likely reflect the large Ln–O bond enthalpy and again, a highly organized/polar transition state.^[7] Intermolecular aminoalkyne hydroamination (Table 7, entry 8) proceeds with ΔH^\ddagger and E_a values slightly larger than most of the intramolecular hydroamination/cyclizations but with a comparably negative ΔS^\ddagger (Table 7, entry 8).^[13c,g,j] The present ΔH^\ddagger and E_a values for Table 7, entry 7 may reflect a transition state in which significant bond formation compensates for bond breaking, with the large negative ΔS^\ddagger consistent with a well-organized, polar transition state and substantial loss of degrees of freedom, not unexpected for an intermolecular process.^[13c]



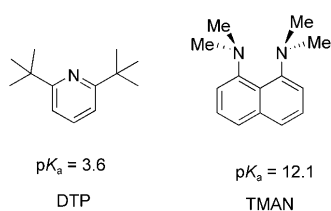
Scheme 5. Proposed catalytic pathways for [Ln(OTf)₃]-mediated intramolecular hydroalkoxylation/cyclization of A) terminal alkenols and alkenols that bear one substituent at the olefin terminus, and B) alkenols that bear two substituents at the olefin terminus.

Table 7. Activation parameter comparison for intra- and intermolecular hydroamination/cyclization and hydroalkoxylation/cyclization processes (Cp' = Cp*, Cp'' = Me₄Cp).

Entry	Substrate	Product	Catalyst	H^\ddagger [kcal mol ⁻¹]	S^\ddagger [eu]	E_a [kcal mol ⁻¹]
1 ^[13b]			[Me ₂ SiCp'' ₂ SmCH(SiMe ₃) ₂]	17.7 (2.1)	24.7 (5)	18.5 (2.0)
2 ^[13f]			[Cp'LaCH(SiMe ₃) ₂]	16.9 (1.3)	16.5 (4)	17.6 (1.4)
3 ^[13j]			[Cp'LaCH(SiMe ₃) ₂]	12.7 (1.4)	27.0 (5)	13.4 (1.5)
4 ^[13g]			[Cp'SmCH(SiMe ₃) ₂]	10.7 (8)	27.4 (6)	11.3 (2.0)
5 ^[14a]			[Cp'SmCH(SiMe ₃) ₂]	12.3 (1.6)	25.9 (5.2)	13.0 (1.4)
6 ^[7]			[La{N(SiCH ₃) ₂ }] ₃	20.2 (1.0)	11.8 (0.3)	20.9 (0.3)
7 ^[a]			[Yb(OTf) ₃]	18.2 (9)	17.0 (1.4)	18.9 (8)
8 ^[13c]			[Me ₂ SiCp'' ₂ NdCH(SiMe ₃) ₂]	17.2 (1.1)	25.9 (9)	17.8 (1.8)

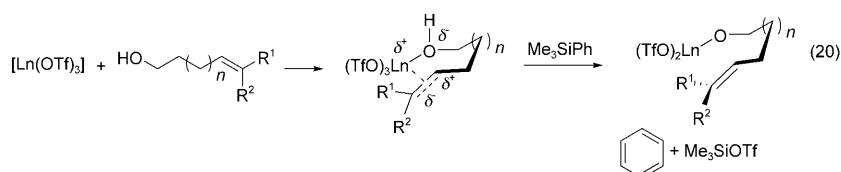
[a] Determined using the catalyst in [C₂mim][OTf].

Investigations with proton traps: Brønsted acids are known catalysts for intramolecular addition of O–H bonds across a pendant olefin.^[4] Thus, detailed characterization of the role of electrophilic Ln metal species in this catalytic transformation must include an understanding of potential proton participation. In principle, this issue may be difficult to probe, since standard mechanistic tests for Brønsted acid involvement include addition of hindered amines (“proton sponges”), which might inhibit product formation for variety of reasons. In the present study, the proton sponges 2,6-di-*tert*-butylpyridine (DTP) and 1,8-bis(dimethylamino)naphthalene (TMAN), which exhibit large differences in relative base strength (pK_a =3.6 and 12.1, respectively)^[39a,d] were



employed. The results reveal that the two sponges affect the HO/cyclization rates differently. [Yb(OTf)₃]-mediated cyclization of **1** in the presence of TMAN (0.5 equiv with respect to [Ln(OTf)₃]) exhibits a significantly slowed reaction rate, whereas negligible HO/cyclization is observed in the presence of 1.0, 2.0, and 3.0 equiv of DTP (Figure 4).

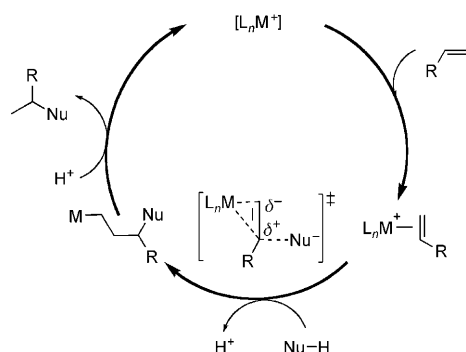
Comparative studies of [Ln(OTf)₃]- and TfOH-catalyzed (**1** and 3 mol %, respectively) **1**→**2** HO/cyclization in the presence of TMAN are informative. For [Yb(OTf)₃]-mediated **1**→**2** cyclization, low TMAN concentrations marginally affect N_t values; only upon the addition of 3.0 equiv of TMAN is cyclization completely inhibited (Figure 4). For TfOH-mediated **1**→**2** hydroalkoxylation/cyclization, incremental TMAN addition (0.5–3.0 equiv) decreases the rate monotonically (Figure 4). These trapping experiments indicate that proton sponges affect [Yb(OTf)₃]- and TfOH-mediated cyclization rates differently, plausibly reflecting the differing steric and basicity characteristics of the two sponges.^[39] To better understand the origin of the proton sponge results, non-nucleophilic proton traps that react rapidly and irreversibly with H⁺ were also employed.^[38,40] It is found that Me₃SiPh inhibits the HO/cyclization process and deactivates the catalyst stoichiometrically. Furthermore, a stoichiometric mixture of Me₃SiPh and **3** remains unchanged after 12 h under identical conditions. The totality of the H⁺ scavenging results suggest that the Ln³⁺ center facilitates intramolecular H⁺ transfer by withdrawing the electron density from the alkenol hydroxyl functionality, thus rendering the O–H proton more acidic and susceptible to transfer [e.g., Eq. (20)]. Analogous results have been observed for a Pt-mediated hydroamination process.^[39]



In addition to these studies, ^{19}F NMR spectroscopic analysis of the volatiles vacuum transferred (with heating) from preparative-scale $[\text{Ln}(\text{OTf})_3]$ - and TfOH -mediated 2-allyl phenol HO/cyclizations reveals the presence of the TfOH only in the case of the latter reactions (see the Experimental Section). These results argue that in $[\text{Ln}(\text{OTf})_3]$ -mediated cyclizations, free TfOH is not formed in any significant quantities during the catalytic cycle. These proton-scavenging results indicate the H^+ transferred originates in the alkenol hydroxyl functionality, and that lanthanide triflates do not serve as precursors of free TfOH . The results are also consistent with reports that metal triflates do not form significant quantities of TfOH in the presence of alcohols.^[41]

Although the aforementioned H^+ trapping experiments suggest proton involvement in the catalytic cycle, other possible alkenol deprotonation pathways may be responsible for the decreased turnover frequencies. If the role of the electron-deficient Ln^{3+} center is to activate the hydroxyl functionality through oxygen coordination, H^+ abstraction by basic amines would yield Ln -alkoxide complexes, thereby inhibiting catalytic turnover. The plausible alternative for lanthanide-mediated alkenol HO/cyclization is through olefin insertion into $\text{Ln}-\text{O}$ bond, as in Scheme 1.^[7] As previously noted, homoleptic lanthanide amido complexes serve as lanthanide-alkoxide precursors.^[7] However, bonding-energetic estimations^[18] (Scheme 1) indicate that the very large $\text{Ln}-\text{O}$ bond enthalpy^[18a,c] renders the olefin insertive step *i* (Scheme 1) significantly endothermic for olefinic alcohols, thus explaining why intramolecular alkenol HO/cyclization is not observed for these catalysts.^[7] These observations in conjunction with the H^+ scavenging results provide a reasonable explanation why HO/cyclization is inefficient for lanthanide alkoxide catalysts.

The activation process for intramolecular HO/cyclization processes depends on the nature of the catalyst center, which can activate either the hydroxyl or $\text{C}=\text{C}$ functionality to varying degrees, thereby resulting in either Markovnikov or anti-Markovnikov regioselectivity.^[4,5,7-15] The most commonly invoked pathway for late-transition-metal-catalyzed nucleophilic addition to olefins that yields Markovnikov regioselection products (Scheme 6) begins with formation of metal-bound olefin, which slips from η^2 to η^1 coordination



Scheme 6. Catalytic addition of NuH to an alkene by outer-sphere nucleophilic attack and subsequent $\text{M}-\text{C}$ bond protonolysis.

upon nucleophilic attack. This pathway may involve the formation of sterically hindered β -carbocationic species, with positive charge buildup favoring the more substituted carbon atom, which is generally the site of nucleophilic attack.^[47]

Coordinative probing of the Yb^{3+} -alkenol interaction: Lanthanides are hard Lewis acids and their interaction with ligands is almost exclusively electrostatic due to shielding of the f orbitals. In contrast to π -backbonding-capable transition metals, lanthanides do not engage in extensive, perhaps requisite, metal-olefin backbonding. However, transitory lanthanide-olefin complexes are frequently invoked in pathways for insertion processes,^[7,13-15] and Ln^{2+} -olefin complexation has been detected spectroscopically using an unsaturated, paramagnetic $4f^7$ NMR spectroscopic probe.^[18a] Thus, in the present study, the viability of Ln^{3+} -olefin coordination was also examined.

For Yb^{3+} , strong spin-orbit coupling results in rapid electron spin-lattice relaxation, thus resulting in reasonably sharp ligand NMR spectroscopic linewidths but expectation of substantial dipolar shifts.^[48] Analysis of the $[\text{Yb}(\text{OTf})_3]$ -mediated **15**→**16** hydroalkoxylation/cyclization reaction mixture reveals a significant upfield displacement of the olefinic ($\Delta \approx 0.12$ ppm; Figure 5a–c, j) and α -carbon ^1H resonances ($\Delta \approx 0.62$ ppm; Figure 5f) versus the 1,1,2,2-tetrachloroethane internal standard. The upfield displacement of the ^1H resonances that result from Ln^{3+} -alkenol functionality interactions likely arises from both dipolar (through space) and contact (through bond) mechanisms.^[17a,48] Ln^{3+} -alkoxide interactions plausibly labilize the $-\text{OH}$ proton for intramolecular transfer to the Ln^{3+} -polarized olefin (see Scheme 5A, step *ii*; Scheme 5B, step *ii*).

Mechanistic recapitulation: In formulating a HO/cyclization scheme that accommodates the mechanistic observations, it is useful to briefly summarize the results. 1) Ln ion-size effects on rates generally follow the Ln contraction with the most Lewis acidic Ln^{3+} centers being the most efficient. 2) Substrate rate sensitivity generally parallels other hydroelementation/cyclization processes. 3) Cyclizations proceed with Markovnikov-type selectivity. 4) Kinetics are first-order in catalyst and substrate over a wide concentration and conversion range. 5) ΔH^\ddagger , ΔS^\ddagger , and E_a values suggest a highly organized transition state. 6) $-\text{OH}/-\text{OD}$ labeling experiments establish regiospecific delivery of a single D to the less-substituted olefinic position with a primary KIE of 2.48 (9). 7) Proton-scavenging experiments that employ nucleophilic and non-nucleophilic proton traps suggest participation of an acidic proton in the catalytic cycle that originates from the hydroxyl functionality, and they show that Ln triflates do not serve as precursors of free triflic acid in significant amounts. 8) Coordinative probing experiments are indicative of hydroxyl and olefin coordination to Yb^{3+} .

Observations 1 to 8 argue for irreversible Ln^{3+} -facilitated intramolecular H^+ transfer to a less-substituted olefinic position to generate a partially or fully carbocationic transition

state. The charge developed is then quenched by alkoxide nucleophilic attack and ring closure to generate a Ln^{3+} -cyclic ether complex. The heterocyclic product then dissociates, thereby restoring the active catalytic species (Scheme 5A, B).

Conclusion

Lanthanide triflates are efficient catalysts for the intramolecular hydroalkoxylation/cyclization of unactivated primary/secondary and aliphatic/aromatic alkenols in room temperature ionic liquids to yield the corresponding furan, pyran, spirobicyclic furan, spirobicyclic furan/pyran, benzofuran, and isochroman derivatives. Cyclizations of diverse alkenols proceed with near-quantitative conversions and reasonably large turnover frequencies. The final products can be isolated either by simple diethyl ether extraction or by vacuum transfer, thus allowing efficient catalyst and ionic liquid recycling. Overall, the present results obtained from the kinetic studies (i.e., rate law, activation parameters, isotope effects) and from structural factors that affect cyclization rates (i.e., metal-ion size, product ring size, substrate-substituent effects) support the general scenario shown in Scheme 5. Final product regioselectivities along with kinetic and mechanistic studies implicate turnover-limiting Ln^{3+} -alkenol complexation, in concert with intramolecular H^+ transfer and alkoxide nucleophilic attack/ring closure.

Experimental Section

Materials and methods: All manipulations of reagents were carried out with rigorous exclusion of O_2 and H_2O in flame- or oven-dried Schlenk-type glassware on a dual-manifold Schlenk-line, or interfaced to a high-vacuum line (10^{-6} torr), or in a N_2 -filled Vacuum Atmospheres glove box with a high-capacity recirculator (<1 ppm O_2). Argon (Matheson, prepurified) was purified by passage through an MnO oxygen-removal column and a Davison 4A molecular sieve column. $[\text{D}_3]\text{Nitromethane}$ (Cambridge Isotope Laboratories) used for NMR spectroscopy-scale reactions, was predistilled under the reduced pressure, dried over CaCl_2 , and stored over activated Davison 4A molecular sieves in vacuum-tight storage flasks under Ar. Pentane was dried using activated alumina columns.^[49] THF was distilled from Na/benzophenone ketyl. D_2O (Cambridge Isotope Laboratories; all 99+ atom % D) was used as received. Substrates **1**, **3**, **7**, **19**, and **39** were purchased from Aldrich Chemical Co., distilled under the reduced pressure, and dried as appropriate prior to use. Substrates **5**,^[7a] **9**,^[50] **11**,^[5d] **13**,^[5d] **15**,^[5a] **17**,^[51] **21**,^[52] **23**,^[53] **25**,^[54] **27**,^[55] **29**,^[5d,56] **31**,^[51] **35**,^[57] **37**,^[58] **41**,^[59] and **43**^[60] were prepared as reported in the literature. All liquid substrates were transferred twice from freshly activated molecular sieves and were freeze-pump-thaw degassed. They were then stored in vacuum-tight storage flasks. Solid substrates were purified by column chromatography, dried under high vacuum, and stored in the glove box before use. $[\text{Ln}(\text{OTf})_3]$ complexes ($\text{Ln} = \text{La}$, Sm , Nd , Yb , and Lu) were prepared according to published procedures.^[61] The ^1H NMR spectroscopic integration internal standard, 1,1,2,2-tetrachloroethane, was purchased from Aldrich Chemical Co., distilled under reduced pressure, and stored under N_2 in a vacuum-tight storage flask before use. The ^{19}F NMR spectroscopic integration internal standard, fluorotrichloromethane, was purchased from Aldrich Chemical Co. (distilled, sure-seal) and used as received. RTILs were prepared and dried according to published procedures,^[62] and were stored in the glove box.

Physical and analytical measurements: NMR spectra were recorded using Varian Inova-500 (FT; 500 MHz, ^1H ; 100 MHz, ^{13}C), Inova-400 (FT; 400 MHz, ^1H ; 100 MHz, ^{13}C), Mercury-400 (FT; 400 MHz, ^1H ; 100 MHz ^{13}C ; 76.7 MHz, ^2H ; 376.9 MHz, ^{19}F), or Bruker Advance III-500 NMR (FT; 500 MHz, ^1H ; 100 MHz, ^{13}C) spectrometers. Chemical shifts (δ) for ^1H , ^2H , and ^{13}C are referenced to internal solvent resonances unless stated otherwise. Chemical shifts (δ) for ^1H , ^2H , and ^{13}C are referenced to internal solvent resonances. Chemical shifts (δ) for ^{19}F are referenced with respect to CFCl_3 ($\delta = 0.00$ ppm) in $[\text{D}_3]\text{nitromethane}$. NMR spectroscopic experiments on air-sensitive samples were conducted in Teflon valve-sealed J-Young tubes. Mass spectral data were obtained using a Varian 1200 Quadrupole mass spectrometer. Elemental analyses were performed by Midwest Microlabs, Indianapolis, IN.

Compound 33: Dimethyl allylmalonate (1.40 g, 0.00781 mol) was added dropwise to a suspension of NaH (0.0162 mol) in THF (30 mL) at 0°C . After the addition was complete, the mixture was allowed to warm to room temperature and stirred for 1 h. The reaction mixture was then cooled to 0°C , and 4-chloro-2-methyl-2-butene (0.0324 mol) in THF (10 mL) was added dropwise. The reaction mixture was then allowed to warm to room temperature and stirred for additional 16 h. The reaction was next quenched with 1 M HCl at 0°C , and the organic material was extracted with diethyl ether. The combined organic extracts were washed with 1 M HCl (2×10 mL), saturated NaHCO_3 (20 mL), and brine (10 mL). The solution was dried over MgSO_4 , filtered, and concentrated. The crude product, 2-allyl-2-(3-methyl-but-2-enyl)malonic acid dimethyl ester, was purified by column chromatography eluting with hexanes/ethyl acetate = 8:2 to yield 1.54 g (0.00636 mol, 81 %) of a colorless oil. Spectral data match the literature.^[4a] ^1H NMR (CD_3NO_2 , 400 MHz): $\delta = 5.74$ – 5.64 (m, 1H), 5.14 – 5.09 (m, 2H), 5.00 (t, $J = 15.2$, 7.6 Hz, 1H), 3.60 (s, 6H), 2.58 (t, $J = 14.8$, 7.2 Hz, 2H), 1.70 (s, 3H), 1.63 ppm (s, 3H).

2-Allyl-2-(3-methyl-but-2-enyl)malonic acid methyl ester (1.54 g, 0.00636 mol) in THF (10 mL) was added dropwise to a suspension of LiAlH_4 (0.0178 mol) in THF (30 mL) at 0°C . The suspension was stirred at room temperature for 1 h then quenched with NaOH (5 mL, 15 mol %) and H_2O (5 mL). The organic material was extracted with diethyl ether and the combined organic extracts were then washed with saturated NaHCO_3 (2×10 mL) and brine (2×10 mL). The ether solution was dried over MgSO_4 , filtered, and concentrated. The crude product was purified by column chromatography eluting with hexanes/ethyl acetate = 8:2 to yield the title compound (1.07 g, 0.00581 mol, 92 %) as a viscous, colorless oil. ^1H NMR (400 MHz): $\delta = 4.01$ – 3.93 (m, 1H), 3.74 – 3.44 (m, 4H), 2.11 – 2.01 (m, 2H), 1.54 – 1.44 (m, 2H), 1.80 (d, $J = 6$ Hz, 3H), 1.58 ppm (d, $J = 6$ Hz, 3H); ^{13}C NMR (100 MHz): $\delta = 134.62$, 133.58, 119.14, 116.5, 66.78, 42.26, 35.42, 29.17, 24.7, 20.45 ppm; elemental analysis calcd (%) for $\text{C}_9\text{H}_{16}\text{O}_2$: C 71.70, H 10.94; found: C 71.67, H 10.91.

General catalytic reaction information: Intramolecular HO/cyclizations of each substrate were first studied as a function of Ln for different $[\text{Ln}(\text{OTf})_3]$ complexes in nitromethane as the solvent. Once the most effective $[\text{Ln}(\text{OTf})_3]$ catalyst was identified for each substrate, the reactions were carried out in ILs.

Preparation of standard solutions for typical NMR spectroscopy-scale catalytic reactions in $[\text{D}_3]\text{nitromethane}$: For each data set, a separate standard solution was prepared under an inert atmosphere in a three-neck round-bottomed flask interfaced to the high-vacuum line. The solution consisted of $[\text{D}_3]\text{nitromethane}$, an internal NMR spectroscopic standard, and the appropriate alkenol (20 equiv per $[\text{Ln}(\text{OTf})_3]$).

Typical NMR spectroscopy-scale catalytic reaction in $[\text{D}_3]\text{nitromethane}$: In the glove box, a J-Young NMR spectroscopy tube equipped with a Teflon valve was charged with a $[\text{Ln}(\text{OTf})_3]$ ($\text{Ln} = \text{La}$, Sm , Yb) catalyst (5 mol %; 1.6×10^{-5} mol). On the high-vacuum line, the tube was evacuated (10^{-6} torr), then frozen at -78°C , followed by addition of the substrate standard solution (700 μL , 20 equiv per Ln^{3+} , $[\text{substrate}] = 0.457$ M) through a gas-tight syringe to the NMR spectroscopy tube under an argon flush. The tube was then evacuated and backfilled with Ar while frozen at -78°C , and then sealed with the Teflon valve. The frozen reaction mixture was maintained in a dry ice/acetone bath until the time for NMR spectroscopic analysis, and then brought to the desired tempera-

ture, and the ensuing hydroalkoxylation/cyclization reaction monitored by ^1H NMR spectroscopy.

Typical small-scale catalytic reaction in RTILs: In the glove box, a 25 mL three-neck round-bottomed flask equipped with a J-Young adapter with a Teflon valve and magnetic stir bar was charged with the $[\text{Ln}(\text{OTf})_3]$ catalyst ($\text{Ln} = \text{La}, \text{Sm}, \text{Nd}, \text{Yb}, \text{and Lu}$; 1 mol%; 1.5×10^{-5} mol), and RTIL (8.9×10^{-3} mol). On the Schlenk line, the flask was evacuated (10^{-3} torr), degassed, and backfilled three times with N_2 while heating gently for approximately 20 min at around 40°C to induce catalyst dissolution in the RTIL. Next, the mixture was heated to the desired reaction temperature (60 – 120°C) and alkenol (1.5×10^{-3} mol, 100 equiv per $[\text{Ln}(\text{OTf})_3]$) was injected through a gas-tight syringe under a nitrogen flush. Upon completion of the reaction, the reaction mixture was cooled to room temperature, and the final product was extracted with small portions of diethyl ether. Final product percent yield was determined directly either by ^1H NMR spectroscopic integration by using a standard solution of 1,1,2,2-tetrachloroethane in $[\text{D}_3]$ nitromethane or after chromatographic product isolation.

Preparative-scale catalytic reaction for $[\text{Yb}(\text{OTf})_3]$ -mediated 1 \rightarrow 2 conversion in $[\text{C}_2\text{mim}][\text{OTf}]$: In the glove box, 1 mol% (1.5×10^{-4} mol) $[\text{Yb}(\text{OTf})_3]$ and $[\text{C}_2\text{mim}][\text{OTf}]$ (8.9×10^{-2} mol) were loaded into a 50 mL three-neck round-bottomed flask equipped with a J-Young adapter with a Teflon valve and magnetic stir bar. On the Schlenk line, the flask was evacuated (10^{-3} torr), degassed, and backfilled three times with N_2 while heating gently for approximately 20 min at around 40°C to induce catalyst dissolution in the RTIL, until the solution became transparent. Next, the mixture was heated to the desired reaction temperature (120°C) and **1** (1.5×10^{-2} mol, 100 equiv per $[\text{Yb}(\text{OTf})_3]$) was injected through a gas-tight syringe under a nitrogen flush. Upon completion of the reaction, the reaction mixture volatiles were removed by means of vacuum distillation. Volatiles removed were analyzed by ^1H and ^{19}F NMR spectroscopy. Final product **2** percent yield was determined by ^1H NMR spectroscopic integration by using a standard solution of 1,1,2,2-tetrachloroethane in $[\text{D}_3]$ nitromethane (1.85 g, 1.38 mmol). ^{19}F NMR spectroscopic analysis of the reaction volatiles (CD_3NO_2 , 376 MHz) removed from reaction mixture by means of vacuum transfer (with heating at 165°C) revealed no detectable triflic acid. In a different trial, a preparative-scale reaction was run to completion. ^{19}F NMR spectroscopic analysis of the vacuum-transferred (with heating) reaction volatiles also revealed no detectable triflic acid.

Preparative-scale catalytic reaction for TfOH-mediated 1 \rightarrow 2 conversion in $[\text{C}_2\text{mim}][\text{OTf}]$: In the glove box, $[\text{C}_2\text{mim}][\text{OTf}]$ (8.9×10^{-2} mol) was loaded into a 50 mL three-neck round-bottomed flask equipped with a J-Young adapter with a Teflon valve and magnetic stir bar. On the Schlenk line, the flask was evacuated (10^{-3} torr), degassed, and backfilled three times with N_2 . Next, 3 mol% (4.5×10^{-4} mol) TfOH was injected under nitrogen, the mixture was heated to the desired reaction temperature (120°C), and **1** (1.5×10^{-2} mol, 33.3 equiv per TfOH) was injected through a gas-tight syringe under a nitrogen flush. Upon completion of the reaction, the reaction mixture volatiles were removed by means of vacuum distillation and were analyzed by ^1H and ^{19}F NMR spectroscopy. Final product **2** percent yield was determined by ^1H NMR spectroscopic integration by using a standard solution of 1,1,2,2-tetrachloroethane in $[\text{D}_3]$ nitromethane (1.72 g, 1.26 mmol). ^{19}F NMR spectroscopic analysis of the reaction mixture volatiles removed by means of vacuum transfer (with heating at 165°C) revealed the presence of triflic acid (CD_3NO_2 , 376 MHz): $\delta = -77.14$ ppm (compared to a chemical shift of commercially available triflic acid).

Compound 18: This compound was obtained by cyclizing **17** (1.5 mmol). ^1H NMR (CD_3NO_2 , 400 MHz; *rac*): $\delta = 4.01$ – 3.93 (m, 2H), 3.74 – 3.44 (m, 4H), 2.11 – 2.01 , 2.11 – 2.01 (m, 2H), 1.54 – 1.44 (m, 2H), 1.80 (d, $J = 6.0$ Hz, 3H), 1.58 ppm (d, $J = 6.0$ Hz, 3H); ^{13}C NMR (CD_3NO_2 , 100 MHz): $\delta = 77.4$, 77.1 , 76.5 , 76.1 , 51.8 , 44.8 , 44.6 , 20.5 , 20.4 ppm; HRMS (ESI): m/z : calcd for $\text{C}_9\text{H}_{16}\text{O}_2$ [M^+]: 156.2256; found 156.2252.

Compound 34: This compound was obtained by cyclizing **33** (1.5 mmol). ^1H NMR (CD_3NO_2 , 400 MHz): $\delta = 3.98$ – 3.87 (m, 1H), 3.79 (d, $J = 8.8$ Hz, 1H), 3.53 – 3.36 (m, 2H), 3.31 (d, $J = 8.8$ Hz, 1H), 1.99 (dd, $J = 12.4$, 6 Hz, 1H), 1.76 (dd, $J = 12.8$, 6.8 Hz, 1H), 1.52 – 1.38 (m, 2H), 1.38 (s, 6H),

1.14 ppm (d, $J = 6.4$ Hz, 3H); ^{13}C NMR (CD_3NO_2 , 100 MHz): $\delta = 75.5$, 74.7 , 70.7 , 68.7 , 67.5 , 43.4 , 43.3 , 34.2 , 30.4 , 20.4 ppm; HRMS (ESI): m/z : calcd for $\text{C}_{11}\text{H}_{21}\text{O}_2$ [M^+]: 185.2875; found 185.2868.

Kinetic studies of hydroalkoxylation/cyclization in $[\text{C}_2\text{mim}][\text{OTf}]$: In a typical experiment, a small-scale reaction was set up as described above (see above). The reaction progress was monitored by withdrawing the aliquots of known mass at preset time intervals. The aliquots were diluted with 1,1,2,2-tetrachloroethane (500 μL) in $[\text{D}_3]$ nitromethane standard solution (see above). For each aliquot, the ^1H NMR spectrum was recorded and integrated versus the internal standard, 1,1,2,2-tetrachloroethane. A long pulse delay was used during data acquisition to avoid saturation.

Reaction order measurements for conversion 1 \rightarrow 2: Kinetics were monitored from ^1H NMR spectroscopic intensity changes in the substrate olefinic resonances over three or more half-lives. The concentration of product **2** was measured from the area of the olefinic peak, standardized to the area of the CH_2 peak of 1,1,2,2-tetrachloroethane in solution. NMR spectroscopic analysis of all reaction mixtures indicates that, within the detection limits, only substrate and product are present in detectable quantities at all stages of conversion. Monitoring substrate consumption as a function of time yields initial rate constants [Eq. (21)]. The data were processed with the SigmaPlot 2000 program.^[63] Turnover frequencies, N_i [h^{-1}], were calculated for the least-squares determined slope (m) according to Equation (19) in which $[\text{catalyst}]_0$ is the initial concentration of the catalyst. Determination of cyclization N_i values for other substrates was carried out in the same way as for cyclization 1 \rightarrow 2.

$$\ln[\text{substrate}] = -mt \quad (21)$$

Activation parameter determination: Eyring and Arrhenius kinetic analyses^[35a,b] of data obtained in variable-temperature experiments for the 15 \rightarrow 16 conversion (see above) were used to extract ΔH^\ddagger , ΔS^\ddagger , and E_a parameters. The errors in these activation parameters were computed from the published error propagation formulas,^[35b] which were derived from the Eyring equation.

Isotopic labeling studies: In the glove box, a 25 mL three-neck round-bottomed flask equipped with a J-Young adapter with a Teflon valve and magnetic stir bar was charged with 1 mol% $[\text{Yb}(\text{OTf})_3]$ catalyst (1.5×10^{-5} mol) and $[\text{C}_2\text{mim}][\text{OTf}]$ (8.9×10^{-3} mol). On the Schlenk line, the flask was evacuated (10^{-3} torr), degassed, and backfilled three times with N_2 while heating gently for approximately 20 min at around 40°C to induce catalyst dissolution. Next, the mixture was heated to the desired reaction temperature (120°C) and $[\text{D}_4]$ 4-penten-1-ol (1.5×10^{-3} mol, 100 equiv per $[\text{Yb}(\text{OTf})_3]$) was injected through a gas-tight syringe under a nitrogen flush. Upon completion of the reaction, the final product was removed by vacuum distillation. Final product percent yield was determined by ^1H NMR spectroscopic integration by using a standard solution of 1,1,2,2-tetrachloroethane in $[\text{D}_3]$ nitromethane. ^2H regioselectivity was determined by integration with respect to $[\text{D}_3]$ nitromethane by utilizing a 5.0% $[\text{D}_3]$ nitromethane in nitromethane.

Mechanistic investigations of $[\text{Yb}(\text{OTf})_3]$ -mediated 1 \rightarrow 2 conversion in $[\text{C}_2\text{mim}][\text{OTf}]$ with proton-trapping reagents

With N,N,N',N' -tetramethyl-1,8-naphthalenediamine: In the glove box, four 25 mL three-neck round-bottomed flasks equipped with a J-Young adapter with a Teflon valve and magnetic stir bar were charged with 1.0 mol% $[\text{Yb}(\text{OTf})_3]$ catalyst (1.5×10^{-5} mol), 0.5, 1.0, 2.0, 3.0 equiv (with respect to $[\text{Yb}(\text{OTf})_3]$) of N,N,N',N' -tetramethyl-1,8-naphthalenediamine, and $[\text{C}_2\text{mim}][\text{OTf}]$ (8.9×10^{-3} mol). On the Schlenk line, the flask was evacuated (10^{-3} torr), degassed, and backfilled three times with N_2 while heating gently for approximately 20 min at around 40°C to induce catalyst dissolution in $[\text{C}_2\text{mim}][\text{OTf}]$. Next, the mixture was heated to the desired reaction temperature (120°C) and **1** (1.5×10^{-3} mol, 100 equiv per $[\text{Yb}(\text{OTf})_3]$) was injected through a gas-tight syringe under a nitrogen flush. Reaction progress was monitored by withdrawing aliquots of known mass at preset times. The aliquots were diluted with 1,1,2,2-tetrachloroethane (500 μL) in the $[\text{D}_3]$ nitromethane standard solution (see above). For each aliquot, the ^1H NMR spectrum was recorded and integrated versus the internal standard, 1,1,2,2-tetrachloroethane. A long pulse delay was used during data acquisition to avoid saturation.

With 2,6-di-tert-butylpyridine: In the glove box, four 25 mL three-neck round-bottomed flasks equipped with a J-Young adapter with a Teflon valve and magnetic stir bar were charged with 1.0 mol % $[\text{Yb}(\text{OTf})_3]$ catalyst (1.5×10^{-5} mol) and $[\text{C}_2\text{mim}][\text{OTf}]$ (8.9×10^{-3} mol). On the dual-manifold Schlenk line, the flasks were evacuated (10^{-3} torr), degassed, and backfilled three times with N_2 while heating gently for approximately 20 min at around 40°C to induce catalyst dissolution in the $[\text{C}_2\text{mim}][\text{OTf}]$, and 2,6-di-tert-butylpyridine (0.5, 1.0, 2.0, and 3.0 equiv with respect to $[\text{Yb}(\text{OTf})_3]$) was added under N_2 flush. Next, the mixture was heated to 120°C and **1** (1.5×10^{-3} mol, 100 equiv with respect to $[\text{Yb}(\text{OTf})_3]$) was injected through a gas-tight syringe under N_2 flush. Reaction progress was monitored by withdrawing aliquots of known mass at a preset time intervals. The aliquots were diluted with 1,1,2,2-tetrachloroethane (500 μL) in the $[\text{D}_3]$ nitromethane standard solution (see above). For each aliquot, the ^1H NMR spectrum was recorded and integrated versus the internal standard, 1,1,2,2-tetrachloroethane. A long pulse delay was used during data acquisition to avoid saturation.

Mechanistic investigation of TfOH-mediated 1→2 conversion in $[\text{C}_2\text{mim}][\text{OTf}]$ using proton-trapping reagents—With *N,N,N',N'*-tetramethyl-1,8-naphthalenediamine: In the glove box, a 25 mL three-neck round-bottomed flask equipped with a J-Young adapter with a Teflon valve and magnetic stir bar was loaded with a *N,N,N',N'*-tetramethyl-1,8-naphthalenediamine (0.5, 1.0, 2.0, 3.0 equiv with respect to TfOH), and $[\text{C}_2\text{mim}][\text{OTf}]$ (8.9×10^{-3} mol). On the dual-manifold Schlenk line, the flask was evacuated (10^{-3} torr), degassed, and backfilled three times with N_2 , and TfOH (3 mol %) was added under N_2 flush. Next, the mixture was heated to 120°C , and **1** (1.5×10^{-3} mol, 33.3 equiv with respect to TfOH), was injected through a gas-tight syringe under N_2 flush. Reaction progress was monitored by withdrawing aliquots of known mass at preset time intervals. The aliquots were diluted with 1,1,2,2-tetrachloroethane (500 μL) in the $[\text{D}_3]$ nitromethane standard solution (see above). For each aliquot, the ^1H NMR spectrum was recorded and integrated versus the internal standard, 1,1,2,2-tetrachloroethane. A long pulse delay was used during data acquisition to avoid saturation.

Mechanistic investigations of $[\text{Yb}(\text{OTf})_3]$ -mediated 3→4 conversion in $[\text{C}_2\text{mim}][\text{OTf}]$ with proton-trapping reagents—With phenyltrimethylsilane: In the glove box, a 25 mL three-neck round-bottomed flask equipped with a J-Young adapter having a Teflon valve and magnetic stir bar was charged with 1.0 mol % $[\text{Yb}(\text{OTf})_3]$ catalyst (1.5×10^{-5} mol), phenyltrimethylsilane (1.0 equiv with respect to $[\text{Yb}(\text{OTf})_3]$), and 8.9×10^{-3} mol $[\text{C}_2\text{mim}][\text{OTf}]$. On the Schlenk line, the flask was evacuated (10^{-3} torr), degassed, and backfilled three times with N_2 while heating gently for approximately 20 min at around 40°C to induce catalyst dissolution in the $[\text{C}_2\text{mim}][\text{OTf}]$. Next, the mixture was heated to the desired reaction temperature (120°C) and **3** (1.5×10^{-3} mol, 100 equiv with respect to $[\text{Yb}(\text{OTf})_3]$) was injected through a gas-tight syringe under N_2 flush. Reaction progress was monitored by withdrawing aliquots of known mass at a preset time intervals. The aliquots were diluted with 1,1,2,2-tetrachloroethane (500 μL) in $[\text{D}_3]$ nitromethane standard solution (see above). For each aliquot, the ^1H NMR spectrum was recorded and integrated versus the internal standard, 1,1,2,2-tetrachloroethane. A long pulse delay was used during data acquisition to avoid saturation. The final reaction mixture was also analyzed by ^{19}F NMR spectroscopy.

Coordinative probing of the Yb^{3+} -olefin interaction: In the glove box, a J-Young NMR spectroscopy tube equipped with a Teflon valve was charged with the paramagnetic ($4f^{13}$) $[\text{Yb}(\text{OTf})_3]$ catalyst (5 mol %, 4.5×10^{-5} mol). On the high-vacuum line, the tube was evacuated to 10^{-6} torr, then frozen at -78°C , followed by addition through a gas-tight syringe of a substrate **15** standard solution (700 μL , 0.457 M, 20 equiv with respect to $[\text{Yb}(\text{OTf})_3]$) in $[\text{D}_3]$ nitromethane under an argon flush. The tube was then evacuated and backfilled with Ar while frozen at -78°C , and then sealed with the Teflon valve. The frozen reaction mixture was maintained in dry ice/acetone bath until the time for NMR spectroscopic analysis. ^1H NMR spectra were recorded at room temperature.

Acknowledgements

We thank the NSF (grant CHE-0809589) for support of this research.

- [1] a) K. Tani, V. Kataoka in *Catalytic Heterofunctionalization*, Vol. 2 (Eds.: A. Togni, H. Grützner), Wiley-VCH, Weinheim, **2001**, pp. 171–216.
- [2] a) M. C. Elliott, E. Williams, *J. Chem. Soc. Perkin Trans. 1* **2001**, 2303–2340; b) Z.-Y. Yao, H.-P. Wu, Y.-L. Wu, *J. Med. Chem.* **2000**, 43, 2484–2487; c) A. Mitchenson, A. Nadin, *J. Chem. Soc. Perkin Trans. 1* **2000**, 2862–2892; d) M. C. Elliott, *J. Chem. Soc. Perkin Trans. 1* **2000**, 1291–1318; e) T. L. B. Boivin, *Tetrahedron* **1987**, 43, 3309–3362; f) P. A. Bartlett, *Tetrahedron* **1980**, 36, 272.
- [3] a) J. Tsuji, *Palladium Reagents and Catalysts*, Wiley, Chichester, **2004**, pp. 27–103; b) T. Pei, X. Wang, R. A. Widenhoefer, *J. Am. Chem. Soc.* **2003**, 125, 648–649; c) K. Muñiz, *Adv. Synth. Catal.* **2004**, 346, 1425–1428; d) Y. Hirai, J. Watanabe, T. Nozaki, H. Yokoyama, S. Yamaguchi, *J. Org. Chem.* **1997**, 62, 776–777; e) M. Rönn, J. E. Bäckvall, P. G. Andersson, *Tetrahedron Lett.* **1995**, 36, 7749–7752.
- [4] For examples of Brønsted acid mediated alkene hydroalkoxylation, see: a) D. C. Rosenfeld, S. Shekhar, A. Tameiyama, M. Utsunomiya, J. F. Hartwig, *Org. Lett.* **2006**, 8, 4179–4182; b) L. Coulombel, E. Duñach, *Green Chem.* **2004**, 6, 499–501; c) B. Wang, Y. Gu, L. Yang, J. Suo, O. Kenichi, *Catal. Lett.* **2004**, 96, 71–74; d) P. J. Linares-Palomino, S. Salido, J. Altarejos, A. Sánchez, *Tetrahedron Lett.* **2003**, 44, 6651–6655.
- [5] For examples of transition-metal-mediated alkene hydroalkoxylation, see: a) C.-G. Yang, C. He, *J. Am. Chem. Soc.* **2005**, 127, 6966–6967; b) Y. Oe, T. Ohta, Y. Ito, *Synlett* **2005**, 179–181; c) Y. Oe, T. Ohta, Y. Ito, *Chem. Commun.* **2004**, 1620–1621; d) H. Qian, X. Han, R. A. Widenhoefer, *J. Am. Chem. Soc.* **2004**, 126, 9536–9537; e) E. Marotta, E. Foresti, T. Marcelli, F. Peri, P. Righi, N. Scardovi, G. Rosini, *Org. Lett.* **2002**, 4, 4451–4453; f) K. Hori, H. Kitagawa, A. Miyoshi, T. Ohta, T. I. Furukawa, *Chem. Lett.* **1998**, 1083–1084; g) K. Hori, H. Kitagawa, A. Miyoshi, T. Ohta, T. I. Furukawa, *Chem. Lett.* **1998**, 1083–1084.
- [6] For examples of metal-triflate-mediated alkene hydroalkoxylation, see: a) K. Komeyama, T. Morimoto, Y. Nakayama, K. Takaki, *Tetrahedron Lett.* **2007**, 48, 3259–3261; b) L. Coulombel, M. Rajzmann, J.-M. Pons, S. Olivero, E. Duñach, *Chem. Eur. J.* **2006**, 12, 6356–6365; c) C.-G. Yang, N. W. Reich, C. He, *Org. Lett.* **2005**, 7, 4553–4556; d) C.-G. Yang, N. W. Reich, Z. Shi, C. He, *Org. Lett.* **2005**, 7, 4553–4556.
- [7] For examples of lanthanide-mediated alkyne and allene hydroalkoxylation, see: a) S. Seo, X. Yu, T. J. Marks, *J. Am. Chem. Soc.* **2009**, 131, 263–276; b) X. Yu, S. Seo, T. J. Marks, *J. Am. Chem. Soc.* **2007**, 129, 7244–7245; c) S. Seo, T. J. Marks, *Chem. Eur. J.* **2010**, in press DOI: 10.1002/chem.200903027.
- [8] a) F. Alonso, I. P. Beletsaya, M. Yus, *Chem. Rev.* **2004**, 104, 3079–3159; b) M. A. Tius in *Modern Allene Chemistry*, Vol. 2 (Eds.: N. Krause, A. S. K. Hashmi), Wiley-VCH, Weinheim, **2004**, pp. 834–838; c) P. A. Bartlett in *Asymmetric Synthesis*, Vol. 3 (Ed.: J. D. Morrison), Academic Press, New York, **1984**, p. 455.
- [9] Baldwin 3- to 7-membered ring-closure rules: a) J. E. Baldwin, *J. Chem. Soc. Chem. Commun.* **1976**, 734–735; b) J. E. Baldwin, R. C. Thomas, L. I. Kruse, L. Silberman, *J. Org. Chem.* **1977**, 42, 3846–3852.
- [10] J. G. Taylor, H. Whithall, K. K. M. Hii, *Chem. Commun.* **2005**, 5103.
- [11] T. Hosokawa, T. Shinohara, Y. Ooka, S.-I. Murahashi, *Chem. Lett.* **1989**, 2001–2004.
- [12] For recent organolanthanide reviews, see: a) S. B. Amin, T. J. Marks, *Angew. Chem.* **2008**, 120, 2034–2054; *Angew. Chem. Int. Ed.* **2008**, 47, 2006–2025; b) H. C. Aspinall, *Chem. Rev.* **2002**, 102, 1807–1850; c) F. T. Edelmann, D. M. M. Freckmann, H. Schumann, *Chem. Rev.* **2002**, 102, 1851–1896; d) G. A. Molander, A. C. Romero, *Chem. Rev.* **2002**, 102, 2161–2186; e) M. Shibasaki, N. Yoshikawa, *Chem. Rev.* **2002**, 102, 2187–2210; f) F. T. Edelmann in *Comprehensive Or-*

- ganometallic Chemistry, Vol. 4 (Eds.: G. Wilkinson, F. G. A. Stone, E. W. Abel), Pergamon Press, Oxford, **1995**, Chapter 2; g) T. J. Marks, R. D. Ernst in *Comprehensive Organometallic Chemistry* (Eds.: G. Wilkinson, F. G. A. Stone, E. W. Abel), Pergamon Press, Oxford, **1982**, Chapter 21.
- [13] For lanthanide-mediated hydroamination, see: a) S. Hong, T. J. Marks, *Acc. Chem. Res.* **2004**, *37*, 673–686; b) J.-S. Ryu, T. J. Marks, F. E. McDonald, *J. Org. Chem.* **2004**, *69*, 1038–1052; c) J.-S. Ryu, Y. Li, T. J. Marks, *J. Am. Chem. Soc.* **2003**, *125*, 12584–12605; d) S. Hong, T. J. Marks, *J. Am. Chem. Soc.* **2002**, *124*, 7886–7887; e) J.-S. Ryu, T. J. Marks, F. E. McDonald, *Org. Lett.* **2001**, *3*, 3091–3094; f) V. M. Arredondo, F. E. McDonald, T. J. Marks, *Organometallics* **1999**, *18*, 1949–1960; g) Y. Li, T. J. Marks, *J. Am. Chem. Soc.* **1998**, *120*, 1757–1771; h) Y. Li, T. J. Marks, *Organometallics* **1996**, *15*, 3770–3772; i) C. M. Haar, C. L. Stern, T. J. Marks, *Organometallics* **1996**, *15*, 1765–1775; j) Y. Li, T. J. Marks, *Organometallics* **1994**, *13*, 439–440; k) M. R. Gagné, C. L. Stern, T. J. Marks, *J. Am. Chem. Soc.* **1992**, *114*, 275–294.
- [14] For lanthanide-mediated hydrophosphination, see: a) A. M. Kawaoaka, M. R. Douglass, T. J. Marks, *Organometallics* **2003**, *22*, 4630–4632; b) M. R. Douglass, M. Ogasawara, S. Hong, M. V. Metz, T. J. Marks, *Organometallics* **2002**, *21*, 283–292; c) M. R. Douglass, C. L. Stern, T. J. Marks, *J. Am. Chem. Soc.* **2001**, *123*, 10221–10238.
- [15] For lanthanide-mediated hydrosilylation and hyboration, see: a) P.-F. Fu, L. Brard, Y. Li, T. J. Marks, *J. Am. Chem. Soc.* **1995**, *117*, 7157–7168; b) K. N. Harrison, T. J. Marks, *J. Am. Chem. Soc.* **1992**, *114*, 9220–9221.
- [16] Y. Li, T. J. Marks, *J. Am. Chem. Soc.* **1998**, *120*, 1757–1771.
- [17] a) S. B. Amin, T. J. Marks, *J. Am. Chem. Soc.* **2007**, *129*, 10102–10103; b) A. M. Kawaoaka, T. J. Marks, *J. Am. Chem. Soc.* **2005**, *127*, 6311–6324; c) V. C. Gibson, S. K. Spitzmesser, *Chem. Rev.* **2003**, *103*, 283–316; d) Y.-X. Chen, T. J. Marks, *Chem. Rev.* **2000**, *100* (special issue on “Frontiers in Metal-Catalyzed Polymerization”).
- [18] a) S. P. Nolan, D. Stern, T. J. Marks, *J. Am. Chem. Soc.* **1989**, *111*, 7844–7853; b) D. F. McMillen, D. M. Golden, *Annu. Rev. Phys. Chem.* **1982**, *33*, 493–532; c) S. W. Benson, *Thermochemical Kinetics*, 2nd ed., Wiley, New York, **1976**, Appendix Tables A10, 11, and 22; d) M. A. Giardello, W. A. King, S. P. Nolan, M. Porchia, C. Sishta, T. J. Marks in *Energetics of Organometallic Species* (Ed.: J. A. Martinho Simoes), Kluwer Academic, Dordrecht, **1992**, pp. 35–54; e) M. R. Gagné, S. P. Nolan, A. M. Seyan, D. Stern, T. J. Marks in *Metal–Metal Bonds and Clusters in Chemistry and Catalysis* (Ed.: J. P. Fackler, Jr.), Plenum Press, New York, **1990**, pp. 113–125; f) T. J. Marks in *Bonding Energetics in Organometallic Compounds* (Ed.: T. J. Marks), ACS Symposium Series 428, American Chemical Society, Washington, DC, **1990**, pp. 1–18; g) S. P. Nolan, D. Stern, D. Hedden, T. J. Marks in *Bonding Energetics In Organometallic Compounds* (Ed.: T. J. Marks), ACS Symposium Series 428, American Chemical Society, Washington, DC, **1990**, pp. 159–174.
- [19] Reviews of [Ln(OTf)₃]-mediated reactions: a) C. J. Li, L. Chen, *Chem. Soc. Rev.* **2006**, *35*, 6882; b) S. Luo, L. Zhu, A. Ralukdar, G. Zhang, X. Mi, J. P. Chen, P. G. Wang, *Mini-Rev. Org. Chem.* **2005**, *2*, 177–202; c) C. Li, *Chem. Rev.* **2005**, *105*, 3095–3165; d) S. Kobayashi, *Chem. Rev.* **2002**, *102*, 2227–2302; e) *Lanthanides: Chemistry and Use in Organic Synthesis, Series: Topics in Organometallic Chemistry, Vol. 2* (Ed.: S. Kobayashi), Springer, Berlin, **1999**, Chapter 2.
- [20] Lanthanide chemistry: a) T. Imamoto, *Lanthanides in Organic Synthesis*, Academic Press, San Diego, **1994**; b) S. Cotton, *Lanthanide and Actinide Chemistry*, Wiley, Chichester, England, **2006**; c) H. C. Aspinall, *Chemistry of f-Elements*, Gordon and Breach Science Publishers, Amsterdam, Netherlands, **2001**; d) *Aqueous-Phase Organometallic Catalysis* (Eds.: B. Cornils, W. A. Herrman), Wiley, New York, **1998**.
- [21] a) G. A. Molander, *Chem. Rev.* **1992**, *92*, 2968; b) G. Lawrence, *Chem. Rev.* **1986**, *86*, 1733.
- [22] [Ln(OTf)₃]-mediated C–C bond-forming reactions: a) S. Kobayashi, I. Hachiya, *J. Org. Chem.* **1994**, *59*, 3590–3596; b) J. B. F. N. Engberts, J. W. Wijnen, *J. Org. Chem.* **1997**, *62*, 2039–2044; c) C. Bellucci, P. G. Cozzi, A. Umami-Ronchi, *Tetrahedron Lett.* **1995**, *36*, 7289–7292.
- [23] C. Reichardt in *Solvents and Solvent Effects in Organic Chemistry*, 3rd ed., Wiley-VCH, Weinheim, **2003**.
- [24] a) *Ionic Liquids IIIB: Fundamentals, Progress, Challenges, and Opportunities*, ACS Symposium Series 902 (Eds.: R. D. Rogers, K. R. Seddon), American Chemical Society, Washington DC, **2005**; b) *Ionic Liquids IIIA: Fundamentals, Progress, Challenges, and Opportunities*, ACS Symposium Series 901 (Eds.: R. D. Rogers, K. R. Seddon), American Chemical Society, Washington DC, **2005**; c) *Ionic Liquids: Industrial Applications to Green Chemistry*, ACS Symposium Series 818 (Eds.: R. D. Rogers, K. R. Seddon), American Chemical Society, Washington DC, **2002**.
- [25] a) V. I. Parvulescu, C. Hardacre, *Chem. Rev.* **2007**, *107*, 2615–2665; b) K. Binnemans, *Chem. Rev.* **2007**, *107*, 2592–2614; c) J. B. Harper, M. N. Kobrak, *Mini-Rev. Org. Chem.* **2006**, *3*, 253–269; d) V. A. Cocalia, K. E. Gutowski, R. D. Rogers, *Coord. Chem. Rev.* **2006**, *250*, 755–764; e) J. Dupont, P. A. Z. Suarez, *Phys. Chem. Chem. Phys.* **2006**, *8*, 2441–2452; f) J. Dupont, R. F. de Souza, P. A. Z. Suarez, *Chem. Rev.* **2002**, *102*, 3667–3692; g) R. Sheldon, *Chem. Commun.* **2001**, *23*, 2399–2407; h) P. Wasserscheid, W. Keim, *Angew. Chem.* **2000**, *112*, 3926–3945; *Angew. Chem. Int. Ed.* **2000**, *39*, 3772–3789; i) T. Welton, *Chem. Rev.* **1999**, *99*, 2071–2083.
- [26] a) T. Singh, A. Kumar, *J. Phys. Chem. B* **2008**, *112*, 12968–12972; b) H. Weingärtner, *Phys. Chem.* **2006**, *220*, 1395–1405; c) F. V. Bright, G. A. Baker, *J. Phys. Chem. B* **2006**, *110*, 5822–5823; d) T. Köddermann, C. Wertz, A. Heintz, R. Ludwig, *Angew. Chem.* **2006**, *118*, 3780–3785; *Angew. Chem. Int. Ed.* **2006**, *45*, 3697–3702; e) C. Wakai, A. Oleinikova, M. Ott, H. Weingärtner, *J. Phys. Chem. A* **2005**, *109*, 17028–17030; f) A. Kawai, T. Hidemori, K. Shibuya, *Chem. Lett.* **2004**, *33*, 1464–1465.
- [27] a) K.-S. Yeung, M. E. Farkas, Z. Qiu, Z. Yang, *Tetrahedron Lett.* **2002**, *43*, 5793; b) J. A. Boon, J. A. Levisky, J. L. Pflug, J. S. Wilkes, *J. Org. Chem.* **1986**, *51*, 480.
- [28] a) S. V. Dzyuba, R. A. Bartsch, *Tetrahedron Lett.* **2002**, *43*, 4657–4659; b) P. Ludley, N. Karodia, *Tetrahedron Lett.* **2001**, *42*, 2011–2014; c) M. J. Earle, P. B. McCormac, K. R. Seddon, *Green Chem.* **1999**, *1*, 2325; d) T. Fisher, A. Sethi, T. Welton, J. Wolf, *Tetrahedron Lett.* **1999**, *40*, 793–796.
- [29] a) C. J. Mathews, P. J. Smith, T. Welton, *Chem. Commun.* **2000**, 1249–1250; b) C. J. Mathews, P. J. Smith, T. Welton, A. J. P. White, D. J. Williams, *Organometallics* **2001**, *20*, 3848–3850.
- [30] a) P. E. Z. Suarez, J. E. L. Dullius, S. Einloft, R. F. de Souza, J. Dupont, *Polyhedron* **1996**, *15*, 1217–1219; b) L. Mußmann, H. Olivier, Y. Chauvin, *Angew. Chem.* **1995**, *107*, 2941–2943; *Angew. Chem. Int. Ed. Engl.* **1995**, *34*, 2698–2700; c) C. E. Song, E. J. Roh, *Chem. Commun.* **2000**, 837–838; d) D. E. Kaufmann, M. Nouroozian, H. Henze, *Synlett* **1996**, 1091–1092.
- [31] A. Dzudza, T. J. Marks, *Org. Lett.* **2009**, *11*, 1523–1526.
- [32] Thorpe–Ingold effect: a) S. M. Bachrach, *J. Org. Chem.* **2008**, *73*, 2466–2468; b) P. G. Sammes, D. J. Weller, *Synthesis* **1995**, 1205–1222.
- [33] a) G. A. Olah, P. V. Reddy, G. K. Prakash, *Chem. Rev.* **1992**, *92*, 6995; b) H. N. C. Wong, M. Y. Hon, C. W. Tse, Y. C. Yip, J. Tanko, T. Hudlicky, *Chem. Rev.* **1989**, *89*, 165–198; c) M. Brookhart, W. B. Studabaker, *Chem. Rev.* **1987**, *87*, 411–432.
- [34] R. D. Shannon, *Acta Crystallogr. Sect. A* **1976**, *32*, 751–767.
- [35] a) S. W. Benson, *Thermochemical Kinetics*, 2nd ed., Wiley, New York, **1986**, pp. 810; b) P. J. Robinson, *J. Chem. Educ.* **1978**, *55*, 509510; c) P. M. Morse, M. D. Spencer, S. R. Wilson, G. S. Girolami, *Organometallics* **1994**, *13*, 1646–1655.
- [36] Parameters in parentheses represent three values derived from the least-squares fit.
- [37] a) R. P. Bell, *The Proton in Chemistry*, 2nd ed., Cornell University Press, Ithaca, New York, **1973**, Chapter 12; b) L. Melander, W. H. Saunders, Jr., *Reaction Rates of Isotopic Molecules*, Wiley, New York, **1980**.
- [38] J. L. McBe, A. T. Bell, D. T. Tilley, *J. Am. Chem. Soc.* **2008**, *130*, 16562–16571.

- [39] For proton traps, see: a) T. Saupe, H. A. Staab, *Angew. Chem.* **1988**, *100*, 895–909; *Angew. Chem. Int. Ed. Engl.* **1988**, *27*, 865–1008; b) R. W. Alder, M. R. Bryce, N. C. Goode, *J. Chem. Soc. Perkin Trans. 2* **1982**, 477–483; c) A. Awwal, F. Hibbert, *J. Chem. Soc. Perkin Trans. 2* **1982**, 1589–1592; d) B. Kanner, H. C. Brown, *J. Am. Chem. Soc.* **1966**, *88*, 986–992.
- [40] a) M. H. Alizadeh, H. Razavi, F. F. Bamoharram, K. Daneshvar, *J. Mol. Catal. A* **2003**, *206*, 89–93; b) A. Alvanipour, C. Eaborn, D. R. M. Walton, *J. Organomet. Chem.* **1980**, *201*, 233–247; c) R. W. Bott, C. Eaborn, P. M. Greasley, *J. Chem. Soc.* **1964**, 4804–4806.
- [41] B. Xu, M. Shi, *Org. Lett.* **2002**, *4*, 2145–2148.
- [42] a) C. K. Ingold, *Structure and Mechanism in Organic Chemistry*, 2nd ed., Bell, London, **1969**; b) E. D. Hughes, C. K. Ingold, *J. Chem. Soc.* **1935**, 244; c) E. D. Hughes, *Trans. Faraday Soc.* **1941**, *37*, 603–631; d) E. D. Hughes, C. K. Ingold, *Trans. Faraday Soc.* **1941**, *37*, 657–685; e) K. A. Cooper, M. L. Dhar, E. D. Hughes, C. K. Ingold, B. J. MacNulty, L. I. Woolf, *J. Chem. Soc.* **1948**, 2043–2049.
- [43] J. L. Anderson, J. Ding, T. Welton, D. W. Armstrong, *J. Am. Chem. Soc.* **2002**, *124*, 14247–14254.
- [44] For Ln^{3+} -arene complexes, see: a) H. Liang, Q. Shen, J. Guan, Y. Lin, *J. Organomet. Chem.* **1994**, *474*, 113–116; b) G. B. Deacon, *Aust. J. Chem.* **1990**, *43*, 1245–1257; c) B. Fan, Q. Shen, Y. Lin, *J. Organomet. Chem.* **1989**, *376*, 6166; d) B. Fan, Q. Shen, Y. Lin, *J. Organomet. Chem.* **1989**, *377*, 5158; e) A. Cotton, W. Schwotzer, *Organometallics* **1987**, *6*, 1275–1279; f) A. Cotton, W. Schwotzer, *J. Am. Chem. Soc.* **1986**, *108*, 4657–4568.
- [45] a) A. Motta, I. L. Fraga, T. J. Marks, *Organometallics* **2006**, *25*, 5533–5539; b) A. Motta, I. L. Fraga, T. J. Marks, *Organometallics* **2005**, *24*, 4995–5003; c) A. Motta, G. Lanza, I. A. Fraga, T. J. Marks, *Organometallics* **2004**, *23*, 4097–4114; d) A. Motta, G. Lanza, I. L. Fraga, T. J. Marks, *Organometallics* **2004**, *23*, 4097–4104; e) Y. K. Kim, T. Livinghouse, J. E. Bercaw, *Tetrahedron Lett.* **2001**, *42*, 2933–2935.
- [46] a) R. Breslow in *Molecular Rearrangements* (Ed.: P. de Mayo), Interscience, New York, **1963**, pp. 233–294; b) P. H. Mazzocchi, H. J. Tamburin, *J. Am. Chem. Soc.* **1970**, *92*, 7220–7221.
- [47] a) J. Muzart, *Tetrahedron* **2008**, *64*, 5955–6008; b) M. R. Gagné, S. J. Lee, A. R. Chianese, *Angew. Chem.* **2007**, *119*, 4118–4136; *Angew. Chem. Int. Ed.* **2007**, *46*, 4042–4059; c) C. Munro-Leighton, S. A. Delp, E. D. Blue, B. T. Gunnoe, *Organometallics* **2007**, *26*, 1483–1493; d) J. Muzart, *Tetrahedron* **2005**, *61*, 5815–5849; e) *Transition Metals for Organic Synthesis, Vols. 1,2* (Eds.: M. Beller, C. Bolm), Wiley-VCH, Weinheim, **2004**; f) H. Jiao, A. Tillack, J. Seayad, M. Beller, *Angew. Chem.* **2004**, *116*, 3448–3479; *Angew. Chem. Int. Ed.* **2004**, *43*, 3368–3398; g) E. Hahn, *Chem. Eur. J.* **2004**, *10*, 5888–5899; h) L. S. Hegedus in *Transition Metals in the Synthesis of Complex Organic Molecules*, University Science Books, Mill Valley, **1999**; i) T. E. Müller, M. Beller, *Chem. Rev.* **1998**, *98*, 675–704; j) J. P. Collman, L. S. Hegedus, J. R. Norton, R. G. Finke in *Principles and Applications of Organotransition Metal Chemistry* (Ed.: A. Kelly), University Science Books, Mill Valley, **1987**.
- [48] a) I. Bertini, C. Luchinat, *Coordination Chemistry Reviews: NMR of Paramagnetic Substances, Vol. 150* (Ed.: A. B. P. Lever), Elsevier, Netherlands, **1996**, Chapter 19; b) B. R. McGarvey, *Can. J. Chem.* **1984**, *62*, 1349–1355; c) B. R. McGarvey, *J. Chem. Phys.* **1976**, *65*, 955–961; d) W. D. Luke, A. Streitwieser, Jr., *ACS Symp. Ser.* **1980**, *131*, 93–140; e) W. D. Horrocks, Jr., *NMR of Paramagnetic Molecules* (Eds.: G. N. La Mar, W. D. Horrocks, R. H. Holm), Academic Press, New York, **1973**, Chapter 4.
- [49] A. B. Pangborn, M. A. Giardello, R. H. Grubbs, R. K. Rosen, F. J. Timmers, *Organometallics* **1996**, *15*, 1518–1520.
- [50] A. E. Hill, D. C. Link, P. Donndelinger, *J. Org. Chem.* **1981**, *46*, 1177–1182.
- [51] M. Bradley, P. J. May, D. C. Harrowven, *Tetrahedron Lett.* **2003**, *44*, 503–506.
- [52] T. Okazaki, Y. Maeda, T. Sugai, K. Mori, *Tetrahedron* **1985**, *41*, 307–311.
- [53] P. H. Teijón, L. M. Burón, R. R. Clemente, R. R. González, A. Fernández-Mateos, *J. Org. Chem.* **2007**, *72*, 9973–9982.
- [54] P. S. Engel, A. M. Culotta, *J. Am. Chem. Soc.* **1991**, *113*, 2686–2696.
- [55] A. Takemiya, J. F. Hartwig, *J. Am. Chem. Soc.* **2006**, *128*, 6042–6043.
- [56] S. M. Peralá, B. P. Conrad, C. A. Hughey, J. A. Shugart, G. W. Breton, *Molecules* **2001**, *6*, 655–662.
- [57] P. Yates, T. S. Macas, *Can. J. Chem.* **1988**, *66*, 110.
- [58] M. C. Marcotullio, V. Campagna, S. Sternativo, F. Constantini, M. Curini, *Synthesis* **2006**, 2760–2766.
- [59] B. Janza, A. Studer, *Org. Lett.* **2006**, *8*, 1875–1878.
- [60] E. C. Ashby, R. N. DePriest, A. B. Goel, B. Wenderoth, T. N. Pham, *J. Org. Chem.* **1984**, *49*, 3545–3556.
- [61] a) A. Dzudza, T. J. Marks, *J. Org. Chem.* **2008**, *73*, 4004–4016; b) J. L. Pascal, M. M. Hamidi, *Polyhedron* **1994**, *13*, 1787–1792; c) A. Abbasi, P. Lindqvist-Reis, L. Eriksson, D. Sandstrom, S. Lidin, I. Persson, M. Sandstrom, *Chem. Eur. J.* **2005**, *11*, 4065–4077; d) K. Egashira, Y. Yoshimura, H. Kanno, Y. Suzuki, *J. Therm. Anal. Calorim.* **2003**, *71*, 501–508; e) H. Zineddine, M. Hnach, M. Hamidi, *J. Fluorine Chem.* **1998**, *88*, 139–141; f) M. Nakayama, S. Nakamura, N. Yanagihara, *Polyhedron* **1998**, *17*, 3625–3631.
- [62] P. Bonhôte, A.-P. Dias, N. Papageorgiou, M. Kalyansundaram, K. Grätzel, *Inorg. Chem.* **1996**, *35*, 1168–1178.
- [63] SigmaPlot 2000 version 6.0., SPSS Inc, Chicago, IL, **2000**.

Received: August 16, 2009
Published online: February 9, 2010